

The Kinetics and Mechanisms of 1,5-Dihydroflavin Reduction of Carbonyl Compounds and Flavin Oxidation of Alcohols. 2. Ethyl Pyruvate, Pyruvamide, and Pyruvic Acid

Robert F. Williams¹ and Thomas C. Bruice*

Contribution from the Department of Chemistry, University of California at Santa Barbara, Santa Barbara, California 93106.

Received April 5, 1976

Abstract: The time courses for the appearance of lumiflavin-3-acetate (Fl_{ox}) on reaction of 1,5-dihydrolumiflavin-3-acetate (FlH_2) and its N(1) anion (FlH^-) with pyruvamide, ethyl pyruvate, pyruvic acid, and pyruvate anion are quantitatively explained by the reactions of Scheme I. In competitive reactions FlH_2 and FlH^- (FlH_{2T}) react with the carbonyl substrate to yield Fl_{ox} and the *N*(5)-carbinolamine (CA) which goes on to the corresponding imine (Im). This initial process ($Fl_{ox} \leftarrow FlH_{2T} \rightleftharpoons CA_T \rightleftharpoons Im_T$) may be characterized by an initial burst of Fl_{ox} production dependent upon pH and carbonyl substrate. Following this initial phase, Fl_{ox} continues to be formed by two pathways. Return of CA to FlH_{2T} contributes but the principal production of Fl_{ox} occurs via the comproportionation of Fl_{ox} with CA [which is an *N*(5)-alkyl-1,5-dihydroflavin]. Formation of CA and Im during the course of the reaction is supported by their spectral identification (at 355–360 and 500 nm, respectively) and by the quantitative reductive trapping with sodium cyanoborohydride and subsequent conversion of the resultant *N*-alkyl-1,5-dihydroflavin to its aminium cation radical ($\lambda_{max} \sim 585$ nm). The concentration of FlH_{2T} remaining in solution, following the initial burst reaction, has been determined via its rapid conversion to Fl_{ox} by addition of CH_2O or additional substrate. An extended kinetic study was deemed feasible only for pyruvic acid and pyruvate due to the competing hydrolysis of ethyl pyruvate and the observed dimerization of pyruvamide during the time of reaction with FlH_{2T} . The time courses for formation of Fl_{ox} from the reaction of pyruvic acid + pyruvate with FlH_{2T} have been simulated by analog computations employing the differential expressions for the reactions of Scheme II. The rate constants obtained from the analog simulation have been fit to $\log k_{rate}$ vs. pH profiles and k_{rate} vs. substrate concentration plots. For ethyl pyruvate and pyruvamide, selective analog simulation of the time courses for Fl_{ox} production suffice to support the mechanism of Scheme I. The direct reaction of ethyl pyruvate with FlH_{2T} to yield ethyl lactate and Fl_{ox} is first order in reactants. At pH 1 the reduction of pyruvic acid + pyruvate is first order in [pyruvic acid + pyruvate] and $[H_3O^+]$, while at pH 3.3 the reaction is second order in [pyruvic acid + pyruvate] and is $[H_3O^+]$ independent. Mechanisms involving $1e^-$ transfer from 1,5-dihydroflavin species to the carbonyl group of the substrate which involve proton transfer to substrate carbonyl oxygen or its derived anion radical are considered. The reasonableness of radical pair intermediates (e.g., $FlH_{2T} \cdot C-O^-$ and $FlH_{2T} \cdot C-OH$) along the reaction path is established from the observation that the computed standard free energies of formation for these species in the pH range of investigation are less positive by 9 to 14 kcal M^{-1} than ΔG^\ddagger_{expt} . At alkaline pH values the standard free energy for pyruvate + $FlH^- \rightarrow$ lactate + Fl_{ox} is positive, and it has been shown that lactamide at pH 11.6 and lactate at pH 10 reduces Fl_{ox} to FlH^- . The kinetics and mechanism for CA and Im formation and the comproportionation of CA and Fl_{ox} are discussed.

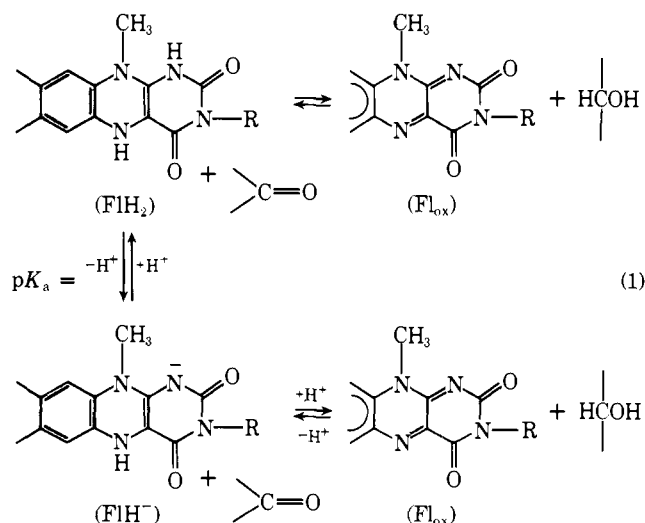
Introduction

An understanding of the mechanisms of flavin mediated redox reactions is of singular importance to the comprehension of the mechanisms of flavoenzyme catalysis.² The reduction of carbonyl compounds by 1,5-dihydroflavins (FlH_2 and FlH^-) and the retrograde oxidation of alcohols by oxidized flavins (Fl_{ox}) serve as important examples of reactions for mechanistic elucidation (eq 1). This manuscript, the second of a series dealing with this topic,³ describes a detailed kinetic study of the 1,5-dihydroflavin reduction of biochemically important pyruvic acid, its amide, and ethyl ester. The results of this study are significant with regard to the mechanistic understanding of lactic acid oxidase. The kinetic findings are discussed in terms of covalent vs. radical mechanisms.^{2,4}

Experimental Section

Materials. 3-Carboxymethyl-7,8,10-trimethylisoalloxazine (I: lumiflavin-3-acetate) was synthesized utilizing the method of Hemmerich⁵ and purified by silica column chromatography. The purity of the lumiflavin-3-acetate was checked by thin-layer chromatography on silica employing two solvent systems (acetic acid/1-butanol/ H_2O 1:2:1 and chloroform/methanol/acetic acid 18:1:1); mp 300 °C dec.

Pyruvic acid (II) was purchased from Aldrich Chemical Co. (Gold Label Lot No. 041647) and carefully purified by distillation at 8 mm Hg. The fraction distilling at 59.0–59.1 °C was collected and stored frozen at –20 °C under nitrogen (lit. bp 65 °C at 10 mm Hg).⁶ **Ethyl pyruvate** (III) from Aldrich (Lot No. 072647) was purified by vacuum



distillation at 68.5 °C at 40 mm Hg (lit. bp 69–71 °C at 42 mm Hg)⁶ and stored at –20 °C. **DL-Lactamide** (IV) was purchased from Sigma Chemical Co. (Lot No. 54C-0222) and purified by two recrystallizations from ethyl acetate to yield a solid melting at 74.5 °C (lit. mp 75.5 °C).⁶ This solid was stored at –20 °C. **Ethyl lactate** (V) from Aldrich was distilled at 153.1–153.9 °C (lit. mp 154 °C)⁶ and stored at –20 °C. **Pyruvamide** (IV) was synthesized by first converting acetyl chloride to pyruvonitrile according to the procedure of Jander and

Scholz (anhydrous hydrogen cyanide in pyridine).⁷ Hydrolysis of the pyruvonnitrile to pyruvamide was cleanly achieved by the passage of dry HCl gas through a solution of pyruvonnitrile in ether (Ankar).⁸ Recrystallization yielded pyruvamide exhibiting a melting point of 123–124 °C (lit. 127 °C,⁸ 123–124 °C⁹). A phenylhydrazone derivative melted at 143–144 °C (lit. 144 °C),¹⁰ the NMR in acetonitrile-*d*₃ exhibited a clean spectra with the methyl resonance at 2.60 ppm, and a uv spectra with a single broad absorbance with a λ_{max} of 343 nm in aqueous solution. No contamination by pyruvic acid could be detected. **Sodium cyanoborohydride**, purchased from Aldrich, was purified according to the procedures outlined by Borch et al.¹¹ and stored under moisture-free nitrogen. **DL-Lactic acid** (Aldrich Gold Label, 99%) was used without further purification. All other salts and buffer materials were analytical reagent grade and were used without further purification.

Methods. All melting points and boiling points are uncorrected. NMR spectra were recorded on a Varian T-60 instrument using Me₄Si as an internal standard. Absorption spectra were recorded on either a Cary 15 or Cary 118C equipped with repetitive-scan, multiple-sample accessories. Kinetic measurements were made on either the Cary 118C or a Gilford 2000 multiple-sample spectrometer. Temperature control was maintained at 30.0 ± 0.1 °C for all kinetic measurements. Solution pH measurements were obtained with a Radiometer Model 26 pH meter equipped with either a Metrohm 9100 or GK-2302C Radiometer combination electrodes equilibrated at 30.0 °C. Measurements of pH were made before and after each kinetic run. Runs were discarded and repeated if drifts in pH of more than 0.2 pH unit occurred.

Deoxygenation of the reaction mixtures was accomplished by passing vanadous-ion scrubbed argon through the reactants in the top and bottom portions of modified Thunberg cuvettes for 30–45 min. Photoreduction (by EDTA) of the lumiflavin-3-acetate to the 1,5-dihydroform was achieved using a 100-W lamp placed at a distance of 10 cm from the Thunberg cuvette. The cuvette was protected from a temperature increase by a water-cooled jacket, and to insure complete reduction the photolysis was continued for 15 min. The spectrum of the reduced material was recorded after the irradiation stopped. Before initiation of the reaction the 1,5-dihydrolumiflavin-3-acetate was monitored (443 nm) for a minimum time period of 20 min to insure complete anaerobicity of the Thunberg.

A Hewlett-Packard 9820A calculator equipped with a 9862A calculator plotter and expanded memory was utilized in the computation of theoretical lines to fit experimental pH–rate profiles and the generation of reaction coordinates. All rate constants were obtained from analog computer fits of the experimental absorbance vs. time data. A 10V EAI TR-20 analog computer equipped with an EAI 1133 variplotter, EAI 6250 digital voltmeter, and an EAI 34.035 repetitive operation display oscilloscope was employed for this purpose.

Kinetic Measurements for the Oxidation of 1,5-Dihydrolumiflavin-3-acetate by Pyruvic Acid. The kinetic measurements were carried out in aqueous solution containing 10 vol % methanol at 30.0 ± 0.1 °C at a calculated ionic strength of 1.0 M (adjusted with KCl) under anaerobic conditions. Typically, 0.5 ml of a methanol stock solution of lumiflavin-3-acetate (7×10^{-4} M) was mixed with 4.0 ml of 1 M KCl solution containing 10^{-3} M EDTA (pH adjusted to desired value) in the bottom of a Thunberg cuvette. Stock pyruvic acid solutions (0.5–5 M) were prepared so that a 0.5-ml aliquot placed in the top of the Thunberg cuvette would yield the final desired concentrations of pyruvic acid (0.1–1.0 M). The pK_a of pyruvic acid is 2.2,^{12,13} so solutions below pH 4 contained no buffer. The pyruvic acid was employed as its own buffer to maintain pH by the addition of HCl or KOH. Above pH 4, 0.085 M acetate or phosphate ($\mu = 1.0$ M) was employed to maintain constant pH. The contents of the Thunberg cuvettes were deoxygenated and the flavin was photoreduced. After the cuvette was examined for oxygen stability, the contents of top and bottom were rapidly mixed to give a solution ca. 7×10^{-5} M in flavin. The appearance of oxidized lumiflavin-3-acetate was recorded at its λ_{max} (443 nm).

Kinetic Measurements for the Oxidation of 1,5-Dihydrolumiflavin-3-acetate by Ethyl Pyruvate and Pyruvamide. The kinetic measurements were carried out in 10 vol % methanol aqueous buffer solutions at 30.0 ± 0.1 °C at a calculated ionic strength of 1.0 M (adjusted with KCl) under anaerobic conditions. A typical example of the reaction of 1,5-dihydrolumiflavin-3-acetate with either carbonyl substrate was as follows: 0.5 ml of a methanolic stock solution of lumiflavin-3-acetate (7×10^{-4} M) was mixed with 4.0 ml of the ap-

propriate buffer solution ($\mu = 1.0$ M) containing 10^{-3} M EDTA in the bottom of a Thunberg cuvette and 0.5 ml of an aqueous buffer solution of the carbonyl substrate ($\mu = 1.0$) was placed in the sidearm of the Thunberg cuvette. The pH's of the solution were measured and adjusted if necessary before introduction into the cuvette. Both top and bottom portions of the cuvette were deoxygenated, and the flavin was photoreduced. After examining the cuvette for oxygen integrity, rapid mixing of the contents of the top and bottom compartment of the Thunberg cuvette resulted in a solution ca. 7×10^{-5} M in flavin, 0.1 M in buffer, and 0.05–0.4 M in carbonyl compound. The appearance of oxidized lumiflavin-3-acetate was recorded at its λ_{max} (443 nm).

Product Analysis of the Reaction of 1,5-Dihydrolumiflavin-3-acetate with Ethyl Pyruvate.¹⁴ An eightfold excess of ethyl pyruvate (9.3 mg, 8×10^{-5} mol) was reacted with 1,5-dihydrolumiflavin-3-acetate (3.14 mg, 1×10^{-5} mol) in an anaerobic aqueous solution (4 ml total volume in a Thunberg cuvette) until the reaction was complete (determined by monitoring at 443 nm). Lypholization of the reaction mixture, followed by thin-layer chromatography on silica containing a fluorescent indicator, yielded good separation of the components. TLC of the aqueous solution without lypholization gave identical results. Two solvent systems were employed, and the R_f values for authentic samples of flavin, ethyl pyruvate, and ethyl lactate were $R_{f\text{CHCl}_3} = 0.05, 0.20, 0.82$ and $R_{f\text{CH}_2\text{CHCl}_2} = 0.05, 0.14, 0.79$, respectively. Examination of the TLC of the reaction mixture showed only three components corresponding to flavin, ethyl pyruvate, and ethyl lactate with $R_f = 0.05, 0.11, 0.74$ in CH₂Cl₂ and $R_f = 0.05, 0.21, 0.82$ in CHCl₃, respectively (see ref 15).

Reduction of Lumiflavin-3-acetate by Lactamide and Lactic Acid. Stock solutions of lactamide or lactic acid (1.0 or 5.0 M) were prepared immediately before use in the appropriate buffer ($\mu = 1.0$ with KCl; phosphate for pH 7–8, borate pH 8–9, carbonate pH 9–10). The stock solution (0.5 ml) was placed in the top of a Thunberg cuvette. In the bottom of the Thunberg cuvette 4.0 ml of a matching buffer solution was mixed with 0.5 ml of a methanolic stock solution of lumiflavin-3-acetate. No EDTA was present in the buffer solutions. After deoxygenating the contents of the cuvette, the top and bottom were rapidly mixed, and the absorbance decrease of oxidized flavin was followed at 443 nm. Typical concentrations in the cuvette were: 7×10^{-5} M lumiflavin-3-acetate, 0.1 M buffer, and 0.1 or 0.5 M in substrate. At the conclusion of the reaction, oxygen was bubbled into the cuvette, and quantitative recovery of the oxidized flavin was observed as long as the pH was 10 or below. Above this pH (experiments with lactamide) concomitant hydrolysis of the flavin was observed.¹⁶

Trapping of Flavin Imine by Sodium Cyanoborohydride. Stock solutions of NaCNBH₃ (1.5×10^{-2} M) in dry methanol were prepared immediately before use. Experiments were performed in either double or single port Thunberg cuvettes. In the bottom of the Thunberg cuvette 4.0 ml of 0.1 M acetate buffer containing 10^{-3} M EDTA ($\mu = 1.0$ M, pH = 5.1) and 0.5 ml stock solution of lumiflavin-3-acetate in methanol (7×10^{-5} M) were mixed. In double port experiments 0.2 ml of aqueous carbonyl compound was placed in one port and 0.2 ml of the NaCNBH₃ solution was placed in the other. Under the pH conditions employed the NaCNBH₃ did not reduce the carbonyl compound, so it was possible to place both substrate and NaCNBH₃ in a single port cuvette. In either case deoxygenation was accomplished by bubbling vanadous-ion scrubbed argon through each cuvette section for 30 min. After photoreduction (EDTA) of the flavin, reactions were initiated by initial addition of either the carbonyl substrate or NaCNBH₃, followed by the other. Final concentrations were: $[\text{Fl}_{\text{ox}}] = 7 \times 10^{-5}$ M, $[\text{EDTA}] = 10^{-3}$ M, $[\text{>C=O}] = 0.1$ M, and $[\text{NaCNBH}_3] = 6 \times 10^{-4}$ M. The reaction was followed by repetitive scanning at the λ_{max} of oxidized flavin (443 nm) or at the λ_{max} of the *N*(5)-alkylflavin product (ca. 345 nm). Addition of oxygen or ninhydrin³ ($\sim 3 \times 10^{-4}$ M in cuvette) generated the *N*(5)-alkylflavin radical species (ca. 585 nm) to establish the production of the *N*(5)-alkyl reduced compound.

Results

The kinetics for oxidation of 1,5-dihydrolumiflavin-3-acetic acid ($\text{FlH}_2 = \text{FlH}^- + \text{FlH}_2$) by ethyl pyruvate, pyruvamide, and pyruvic acid are multiphasic in an unusual manner under all conditions of pH and concentration employed ($\mu = 1.0$ M, 30.0 °C). These reactions are characterized by an initial, rapid

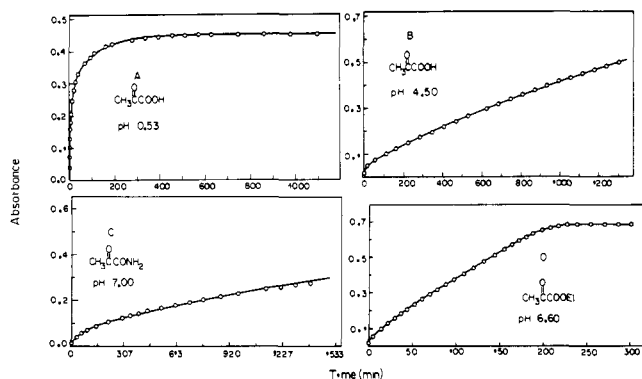
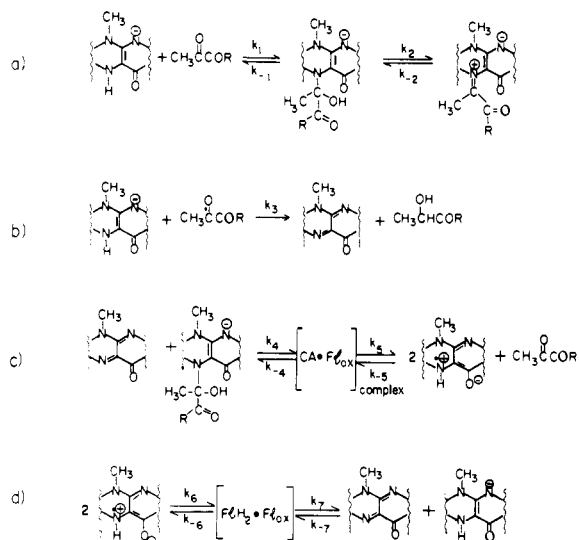


Figure 1. Typical absorbance vs. time plots for the reaction of pyruvic acid, pyruvamide, and ethyl pyruvate (0.10 M) with 1,5-dihydroflumiflavin-3-acetic acid (7.0×10^{-5} M) at 30 °C, $\mu = 1.0$ with KCl. The points are experimental, and the line is the theoretical analog solution of Scheme 11.

(burst) formation of lumiflavin-3-acetate (Fl_{ox}), followed by a continuing but slower formation of Fl_{ox} . The second and slower phase of reaction varies in the order of Fl_{ox} formation from apparent zero order, as previously reported¹⁵ for ethyl pyruvate, to no clear order. The initial burst, depending upon carbonyl compound and pH, may account for a major portion of Fl_{ox} formation or a very minor fraction of Fl_{ox} formation. Figure 1 presents four representative Fl_{ox} (443 nm) vs. time plots for the oxidation of FlH_{2T} by carbonyl compounds. Considerable thought and experimentation leads us to propose the mechanism of Scheme I to account for the kinetics of Fl_{ox}

Scheme I



appearance on reaction of pyruvic acid, ethyl pyruvate, and pyruvamide with FlH_2 and FlH^- (Scheme I has been presented for FlH^- but pertains also to FlH_2). What follows is a presentation of experimental results which support the reactions of Scheme I.

The spectrum obtained immediately after mixing α -keto acid, ester, or amide with dihydroflavin resembles the typical spectrum that has been reported for $N(5)$ -alkylflavins [e.g., 1,5-dihydro-3-methyl-5-ethylflumiflavin has a broad λ_{max} centered at 345 nm (340–360 nm)].¹⁷ A typical spectrum of the reaction of ethyl pyruvate with FlH_{2T} at pH 8.85 (corrected for the absorbance of ethyl pyruvate) is shown in Figure 2. The appearance of a broad peak at ~ 350 nm is observed. The assignment^{15,19} of this spectrum to the $N(5)$ -carbinolamine (CA) of reaction a of Scheme I is reasonable. If oxygen is bubbled

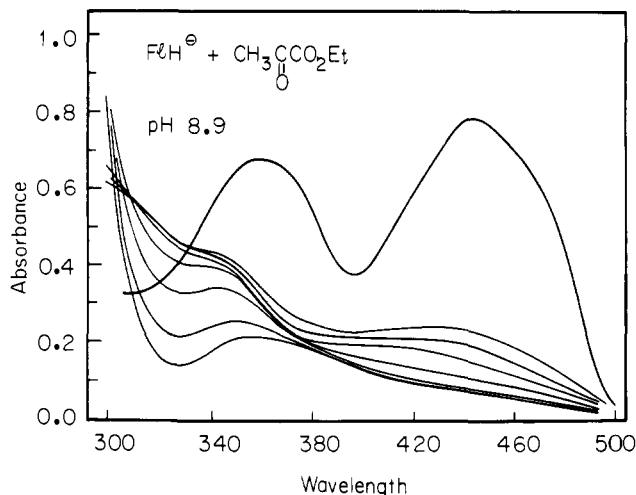


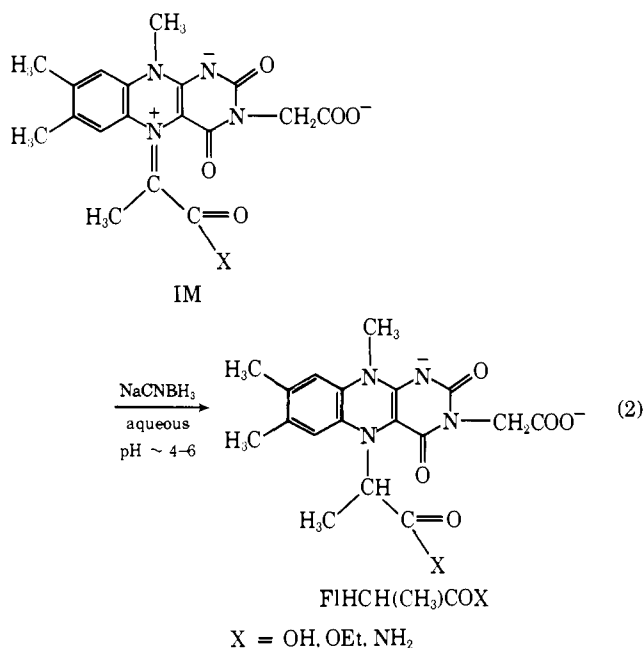
Figure 2. Repetitive scan for the reaction of ethyl pyruvate (0.10 M) with 1,5-dihydroflumiflavin-3-acetic acid (6.5×10^{-5} M) at pH 8.9 (0.1 M borate buffer). The initial scan was recorded 1 min after initiation of reaction. The last scan, before oxygen addition, was recorded 269 min after initiation of reaction. Five minutes of oxygen bubbling produced the normal Fl_{ox} spectrum (top trace). The initial absorbance between 340–360 nm is characteristic of an $N(5)$ -alkyl-1,5-dihydroflavin.

through the solution after completion of the initial burst, ca. 5–10 min are required for complete formation of Fl_{ox} (dependent upon pH and carbonyl compound). The reaction of 3O_2 with 1,5-dihydroflavins is a much more rapid process,²⁰ and the observed slow reoxidation is characteristic of $N(5)$ -alkyl-1,5-dihydroflavins¹⁷ ($t_{1/2} \sim 0.5$ –1 min).²⁰ The oxygen reactivity of 4a-substituted flavins is very much slower¹⁷ (ca. 10^{-4} min⁻¹)¹⁸ than the observed oxidation of the reaction mixture in the dark. Further supporting evidence for the formation of CA compounds will be presented in subsequent papers.^{21,22}

Carbinolamine cannot be an intermediate in the conversion of FlH_{2T} to Fl_{ox} since its rate of formation is commensurate with a decrease (e.g., the end of the initial burst, see Figure 2 and ref 21) in Fl_{ox} production. This result is most clear-cut in the reactions where ethyl pyruvate and pyruvamide are substrates. The characteristic spectrum of a 5-carbinolamine (340–360 nm) is observed when equal concentrations of pyruvic acid are present in the sample and reference cell (λ_{max} 326 nm for pyruvic acid). Spectrum A of Figure 3 exhibits a peak at 360 nm that appears within 6 min after mixing FlH_{2T} with 0.1 M pyruvic acid at pH 0.74. As the reaction proceeds there are absorbance increases at 360, 440, 470, and 515 nm. The spectra A to D of Figure 3 are normalized difference spectra (trace B has been normalized to 1.0 at 443 nm—510 min after initiation of the reaction of pyruvic acid with FlH_{2T}). The appearance of a long wavelength absorption centered at about 515 nm suggests another possible species in solution. Dehydration of the 5-carbinolamine to form an imine would not be unexpected²³ (eq a of Scheme I). A similar imine structure ($X = -OH$, cyclized with the flavin C(4) carbonyl group) has been suggested by Massey and Gibson²⁴ and Hemmerich et al.²⁵ to possess an absorbance at about 500 nm. Such a “red complex” was tentatively assigned to an intermediate in the enzymatic reaction of an α -keto acid with D-amino acid oxidase. The spectrum of Fl_{ox} was normalized to 1.0 at 443 nm and subtracted from curve B of Figure 3, producing curve D. Curve D clearly shows an absorbance at 360 nm (which may be attributed to either a 5-carbinolamine or 4a-adduct) and a broad absorbance centered at 500 nm which can be assigned to the imine structure. A 5-carbinolamine structure corresponding to the 360 nm absorbance is favored over the possible 4a-adduct because of the observed slow oxi-

dation¹⁸ (or no oxidation at all)¹⁷ of authentic 4a-adducts by oxygen. In addition, other carbonyl substrates show absorbances at shorter wavelengths (i.e., formaldehyde and acetaldehyde, $\lambda_{\text{max}} \sim 350 \text{ nm}$).^{20,21} As the pH is decreased, formation of imine is visually perceived. Thus, the color of the solutions becomes more reddish brown. At completion of phase II at the most acidic pH values some imine remains. This can be shown by the fact that less than the expected theoretical yield of Fl_{ox} is obtained unless oxygen is added. There is no observation of irreversible destruction of the flavin.

The possibility of an imine being a direct intermediate in the carbonyl compound oxidation of $\text{FlH}_{2\text{T}}$ to Fl_{ox} had been suggested by Blankenhorn, Ghisla, and Hemmerich.¹⁹ The spectral evidence presented herein (Figure 3) supports the presence of imine. More directly, the imine may be trapped by reduction with sodium cyanoborohydride (eq 2) (Experimental Section). The formation of *N*(5)-alkyl reduced compounds (eq 2) was



quantitated by its spectrum and by its quantitative conversion to the flavin aminium cation radical (blue 585 nm) by oxidation with oxygen or ninhydrin (Experimental Section). Control experiments showed that only at $\text{pH} \leq 4$ did NaCNBH_3 show appreciable reduction of Fl_{ox} to $\text{FlH}_{2\text{T}}$. In performing the trapping experiments, care was exercised in protecting the reaction mixtures from light because an irreversible photochemical reaction (presumably due to reduction of the flavin C(4) carbonyl group)²⁶ occurred when solutions of $\text{FlH}_{2\text{T}}$ or Fl_{ox} plus NaCNBH_3 were exposed to fluorescent light. Since little or no reduction of Fl_{ox} occurred in the dark, it was possible to reduce all imine formed at completion of the initial burst of Fl_{ox} and thereby prevent further formation of Fl_{ox} . The amount of Fl_{ox} formed during the burst and in the presence of NaCNBH_3 corresponds to that predicted (vide infra) from computer fitting of the differential expressions for the reactions of Scheme I to Fl_{ox} production. For example, at $\text{pH} 4.05$ the increase in absorbance at 443 nm (λ_{max} of Fl_{ox}) was 0.013 optical density unit when pyruvic acid was reacted with $\text{FlH}_{2\text{T}}$ in the presence of NaCNBH_3 . The theoretical absorbance increase expected based on the partitioning between k_1 and k_3 (vide infra, see Table IV) is 0.017. Although this change is small it was reproducible and at other pH values reasonable comparisons could also be obtained [at $\text{pH} 3.33$, $\text{OD}_{(\text{expected})} = 0.097$ and $\text{OD}_{(\text{observed})} = 0.083$]. Below $\text{pH} 3$ the NaCNBH_3 is decomposed, and above $\text{pH} 4$ the burst becomes too small

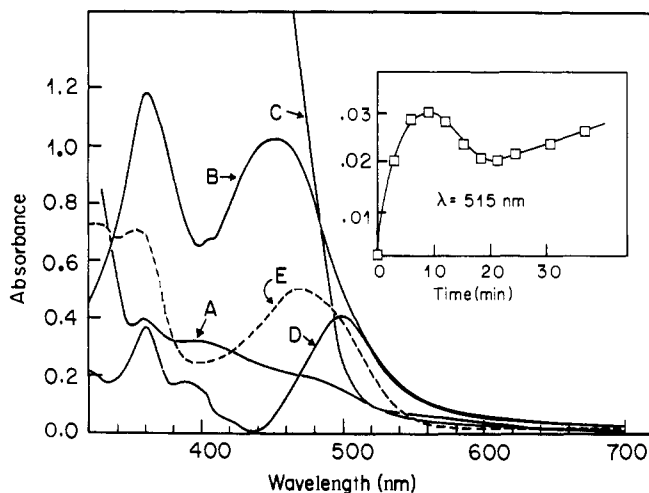


Figure 3. Analysis of the spectral components of the reaction of pyruvic acid (0.10 M) with 1,5-dihydroxylumiflavin-3-acetic acid ($7.0 \times 10^{-5} \text{ M}$) at 30°C , $\mu = 1.0$ with KCl, and $\text{pH} 0.74$. (A) Spectrum observed 6 min after initiation of reaction. The absorbance scale has been adjusted to that of trace B. (B) Spectrum after 510 min of reaction (curve normalized to 1.0 at $\lambda = 442 \text{ nm}$). (C) Spectrum of Fl_{ox} at the end of the reaction relative to trace B. (D) Resultant spectrum obtained by subtraction of the spectrum of Fl_{ox} (normalized to 1.0 at $\lambda = 442 \text{ nm}$) from trace B. (E) Spectrum of $\text{FlH}_{2\text{T}}$ at $\text{pH} 0.74$ (generated by photolysis of a solution of dihydroflavin in the presence of EDTA. Normalized to 0.5 at $\lambda = 468 \text{ nm}$ to show curve shape only).

to accurately measure. Addition of NaCNBH_3 to the reaction mixture after completion of the initial burst always produced the corresponding concentration of reduced *N*-alkylflavin, which, when added to the concentration of Fl_{ox} produced during the burst, accounted for 100% of the starting $\text{FlH}_{2\text{T}}$. These results conclusively establish that the direct pathway for oxidation of $\text{FlH}_{2\text{T}}$ cannot involve CA or Im (Scheme I). However, Im does form with all substrates employed. The decreased rate of Fl_{ox} formation after the initial burst in Fl_{ox} production is logically explained by $\text{FlH}_{2\text{T}}$ being in favorable equilibrium (tied up) with CA and Im.

That the burst reaction represents the competitive conversion of dihydroflavin to oxidized flavins on the one hand and to carbinolamine plus imine on the other (reactions a and b of Scheme I) is supported by experiments which involve the addition of carbonyl compound following the initial burst. In experiments which have appeared in communicative form. Shinkai and Bruce¹⁵ have shown that in the reaction of CH_2O with $\text{FlH}_{2\text{T}}$ the addition of CH_2O following the initial burst does not effect the rate of Fl_{ox} appearance. Thus, although only a fraction of $\text{FlH}_{2\text{T}}$ has been converted to Fl_{ox} at termination of the burst no detectable concentration of dihydroflavin remained. Two similar experiments were performed in this study employing: (1) the addition of ethyl pyruvate to the reaction of $\text{CH}_3(\text{C}=\text{O})\text{COOEt}$ with $\text{FlH}_{2\text{T}}$ after the initial burst (Figure 4) and (2) the addition of formaldehyde to the reaction of $\text{CH}_3(\text{C}=\text{O})\text{COOH}$ with $\text{FlH}_{2\text{T}}$ after the initial burst (Figure 5). Formaldehyde was used to determine free $\text{FlH}_{2\text{T}}$ present after the initial burst because of its more rapid reaction with $\text{FlH}_{2\text{T}}$, as compared with pyruvic acid. Figures 4 and 5 show that addition of carbonyl compound, after completion of the initial burst, provides an increase in the rate of Fl_{ox} formation. The percentages of $\text{FlH}_{2\text{T}}$ remaining in solution at a given time were found to be essentially identical when assayed by either the trapping technique of anaerobic addition of more carbonyl compounds or by analog simulation of A_{443} vs. time plots (vide infra, see Figure 6A-C). When an additional aliquot of ethyl pyruvate was added to the reaction mixture at 300 min (Figure 4), the absorbance increase establishes 11% free $\text{FlH}_{2\text{T}}$ while the analog solution predicts

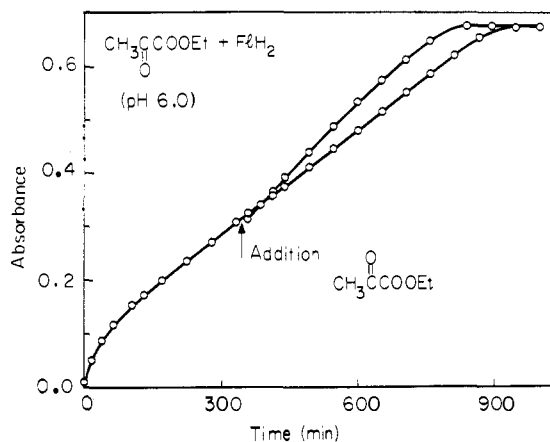


Figure 4. Absorbance vs. time plot for the reaction of ethyl pyruvate (0.10 M) with 1,5-dihydroflumiflavin-3-acetic acid (6.5×10^{-5} M) at 30°C , $\mu = 1.0$ with KCl, and pH 6.0. The arrow indicates the point in time at which the solution was adjusted to 0.15 M in ethyl pyruvate (anaerobically) and shows further reaction of the dihydroflavin present.

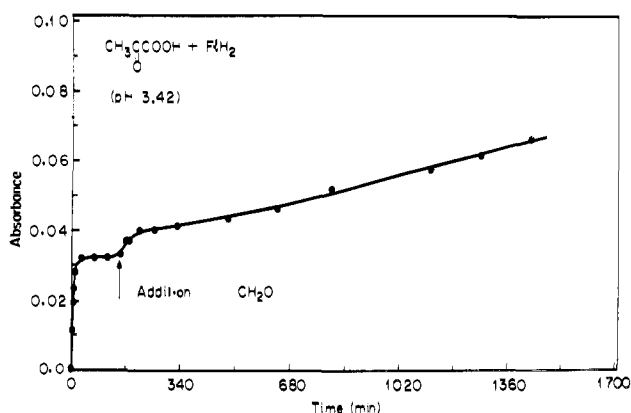


Figure 5. Absorbance vs. time plot for the reaction of pyruvic acid (0.10 M) with 1,5-dihydroflavin-3-acetic acid (3.2×10^{-5} M) at 30°C , $\mu = 1.0$ with KCl, and pH 3.42. The arrow indicates the point in time when an aliquot of CH_2O was added to the reaction mixture (anaerobically). The burst in Fl_{ox} production is due to reaction of CH_2O with remaining dihydroflavin. Final concentrations in the cell were $[\text{FlH}_{2\text{T}}] = 2.9 \times 10^{-5}$ M, $[\text{CH}_2\text{O}] = 0.10$ M, and $[\text{pyruvic acid}] = 0.09$ M.

12.3% free $\text{FlH}_{2\text{T}}$ (Figure 6C). The pyruvic acid reaction (Figure 5) exhibits 7% free $\text{FlH}_{2\text{T}}$ by the addition of formaldehyde while the analog solution shows 8.1% free $\text{FlH}_{2\text{T}}$ (Figure 6B).

The observation (spectral) of transient species, assignable on the basis of λ_{max} values to carbinolamine (CA) and imine

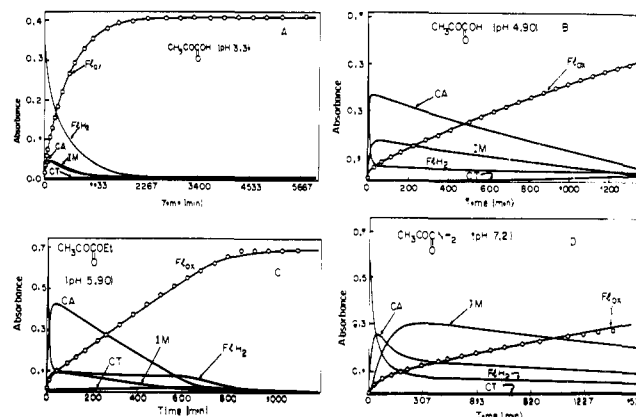
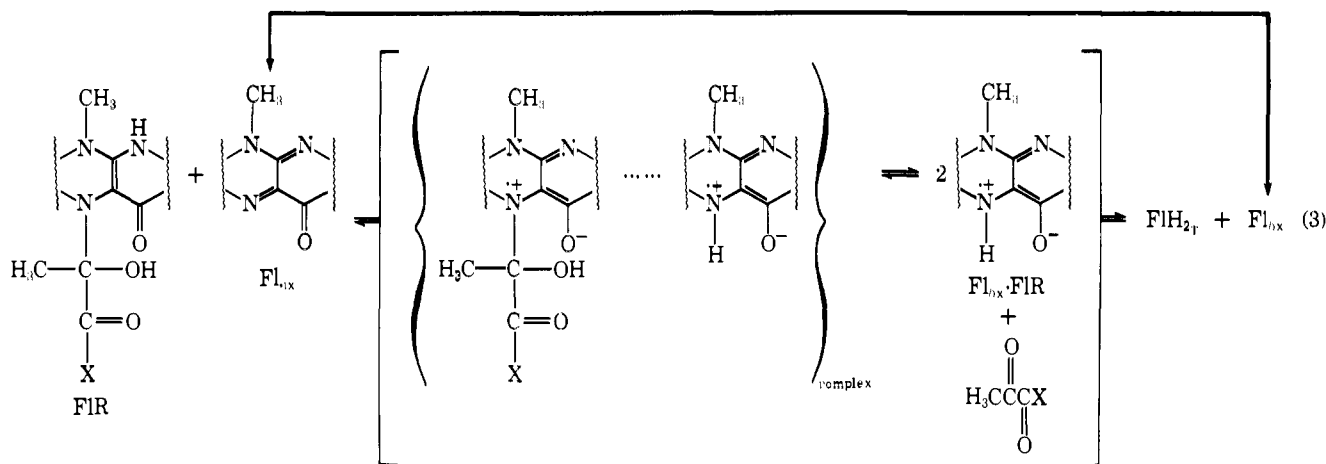


Figure 6. Representative examples of analog computer fittings of Scheme 11 to the formation of Fl_{ox} in the reactions of $\text{CH}_3\text{COCO}_2\text{H}$, $\text{CH}_3\text{COCONH}_2$ and $\text{CH}_3\text{COCO}_2\text{C}_2\text{H}_5$ with 1,5-dihydroflumiflavin-3-acetic acid. The points are experimental, and the solid lines are theoretical for the production and/or disappearance of starting material, intermediates, and products. (A) $[\text{CH}_3\text{COCO}_2\text{H}] = 0.20$ M, $[\text{FlH}_{2\text{T}}] = 3.5 \times 10^{-5}$ M, pH 3.30; (B) $[\text{CH}_3\text{COCO}_2\text{H}] = 0.10$ M, $[\text{FlH}_{2\text{T}}] = 7.0 \times 10^{-5}$ M, pH 4.90; (C) $[\text{CH}_3\text{COCO}_2\text{Et}] = 0.10$ M, $[\text{FlH}_{2\text{T}}] = 6.5 \times 10^{-5}$ M, pH 5.90; (D) $[\text{CH}_3\text{COCO}_2\text{NH}_2] = 0.10$ M, $[\text{FlH}_{2\text{T}}] = 7.0 \times 10^{-5}$ M, pH 7.2.

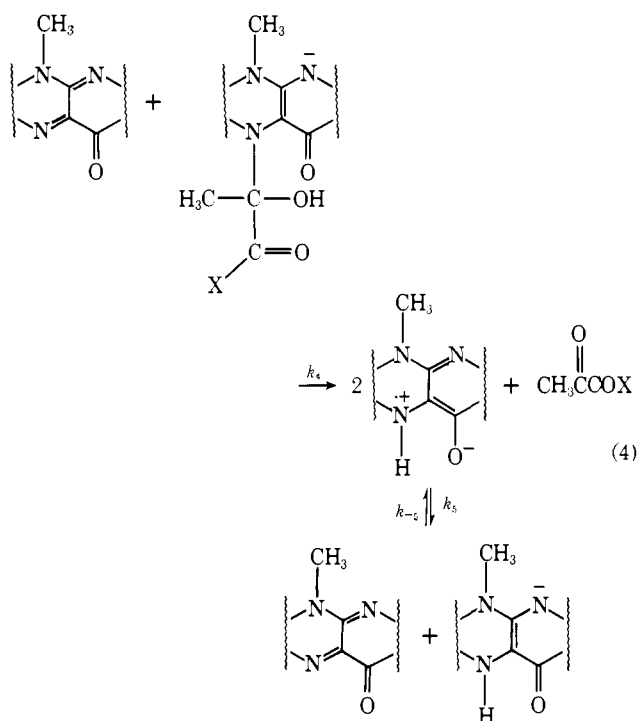
(Im) and the trapping of Im by cyanoborohydride (eq 2) plus the finding that the rate of disappearance of dihydroflavin exceeds the rate of appearance of Fl_{ox} , provides substantial support to the reactions a and b of Scheme I. However, these reactions by themselves do not provide a quantitative description of the time course for Fl_{ox} appearance on reaction of pyruvates with $\text{FlH}_{2\text{T}}$. Thus, analog simulation of the Fl_{ox} absorbance vs. time plots for the reaction of pyruvic acid with $\text{FlH}_{2\text{T}}$ using only reactions a and b of Scheme I provided acceptable results only at acidic pH values. For ethyl pyruvate and pyruvamide, acceptable fits could not be obtained at any pH studied.

On the basis that the 5-carbinolamine (CA) has a formal $N(5)$ -alkyl-1,5-dihydroflavin structure, it would be anticipated that a comproportionation reaction between CA and Fl_{ox} (reaction c of Scheme I) might occur. In separate experiments, and as predicted by the disproportionation mechanism of eq 3, the addition of Fl_{ox} (7.0×10^{-5} and 2.1×10^{-4} M) was shown to catalyze the second slower reaction (by two- to threefold) but to leave the initial burst unaffected (see also ref 21). Attempts to identify the flavin radical species (spectrally) as an intermediate met with limited success. Curve E of Figure 3 depicts the typical spectrum of the flavin aminium cation radical, $\text{FlH}^{\cdot+}$ (normalized to 0.5 at λ_{max} 468 nm to show curve



shape only). Clearly, both the "carbinolamine" and "imine" absorbances could have a flavin radical component during the course of the reaction of pyruvic acid with $\text{FlH}_{2\text{T}}$. Therefore, the production of radicals by comproportionation (reaction c, Scheme I) is consistent with the observed spectral results (similar spectral changes have been observed in an enzymatic system, see Müller et al.²⁶). The inset of Figure 3 is a plot of the absorbance at 515 nm which increases, decreases, and then increases again. The initial increase may be attributed to formation of the flavinium cation radical whose disappearance is followed in time by the first-order formation of imine. Within the time period observed (~ 20 min) the "burst" reaction predominates, and, since the flavin aminium cation radical will contribute at this wavelength, the direct oxidation of $\text{FlH}_{2\text{T}}$ (eq b, Scheme I) would appear to produce the flavin radical cation. A maximum in absorbance at 515 nm is reached as the $\text{FlH}_{2\text{T}}$ partitions between CA (k_1) and Fl_{ox} (k_3). Then a decrease in absorbance follows until the production of imine contributes to the absorbance at 515 nm. Scheme I represents, as we shall see, the minimum set of equations necessary to account quantitatively for all the kinetic observations of this study (and the other studies which will follow).²¹

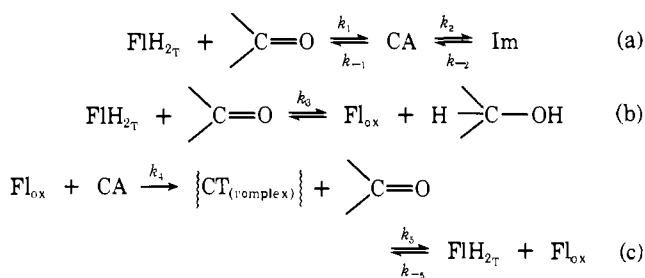
For the purpose of analog simulation of the time dependence for Fl_{ox} appearance, the reactions c and d of Scheme I need not be considered in toto. It has been established,²⁸⁻³⁰ in the comproportionation of other flavins, that the rate of formation of the intermediate dimer from $\text{FlH}_{2\text{T}} + \text{Fl}_{\text{ox}}$ or 2FlH_{T} greatly exceeds dimer dissociation to $\text{FlH}_2 + \text{Fl}_{\text{ox}}$ and 2FlH_{T} . Thus reactions c and d of Scheme I have been replaced by eq 4 to provide Scheme II.



The reaction of ethyl pyruvate, pyruvamide, and pyruvic acid with $\text{FlH}_{2\text{T}}$ exhibits the time dependencies shown in Figure 6A–D for all species in Scheme II. The solution of the differential equations for Scheme II, as generated by the analog computer, provides excellent fits to the experimental points of A_{443} vs. time. This is a most important observation since the validity of this study rests upon the analog simulation of Scheme II to experimental data (see Appendix).

Of the three carbonyl compounds investigated in this study, pyruvic acid has been chosen for the most extensive investigation. Even though the hydration equilibrium is invariant for ethyl pyruvate between pH 2 and 6,³¹ the hydrolysis of the ester

Scheme II



was considered as a likely problem due to the extended time required for reaction with dihydroflavin. For pyruvamide at concentrations >0.1 M there is seen, in the absence of dihydroflavin, a disappearance ($t_{1/2} \sim 3-4$ h) of the pyruvamide absorbance ($\lambda_{\text{max}} 343$ nm). Hydration of pyruvamide may be followed by NMR and is very rapid with an equilibrium constant of ~ 1 .³² The decrease in absorbance was found to be dependent upon $[\text{pyruvamide}]^2$ in accord with a dimerization reaction.³² Though pyruvic acid also undergoes a dimerization reaction, the slowness of this process, even at high pyruvic acid concentrations,³³ assured the unimportance of this reaction in the time period required for its reduction by dihydroflavin. The limited kinetic observations made on the dihydroflavin reduction of ethyl pyruvate and pyruvamide will be presented, followed by the results of the pyruvic acid study.

The reduction of ethyl pyruvate to ethyl lactate¹⁵ by 1,5-dihydroflumiflavin-3-acetic acid at pH 5.9 and 6.6 [$\text{ethyl pyruvate}] = 0.1$ M] is accompanied by the Fl_{ox} appearance time courses of Figure 6C and 1D, respectively. In both figures the points are experimental and the curve computer generated. The apparent rate constants required to fit the curves are included in Table I. The initial burst reaction, in cases where it is large and well defined, can be treated in the ordinary fashion for competitive formation of two products from a single reactant ($k_p = k_1 + k_3$). Following the initial burst, the change of A_{443} with time is virtually a straight line (apparent zero-order production of Fl_{ox}). Extrapolation of this linear plot to $t = 0$ provides an intercept on the absorbance ordinate which equals $k_3/(k_1 + k_3)$ if the simplifying assumption is made that only reactions a and b of Scheme I are in effect. At $\text{FlH}_{2\text{T}} = 6 \times 10^{-5}$ M and ethyl pyruvate at 0.10 M, the ratio $k_3/(k_1 + k_3) = 0.091$ and $k_p = (k_1 + k_3) = 0.127 \text{ min}^{-1}$. Solution of the two simultaneous equations provides $k_3 = 0.116 \text{ M}^{-1} \text{ min}^{-1}$ and $k_1 = 1.15 \text{ M}^{-1} \text{ min}^{-1}$ (ref 15, pH 5.9), while the computer fit to Scheme II provides $k_3 = 0.100 \text{ M}^{-1} \text{ min}^{-1}$ and $k_1 = 8.20 \times 10^{-1} \text{ M}^{-1} \text{ min}^{-1}$ at pH 5.9 (Table I). However, only the rate constants for ethyl pyruvate can be approximated in this manner since the increase in A_{443} with time for pyruvamide or pyruvic acid is not linear following the initial burst. At constant pH, plots of k_p vs. ethyl pyruvate concentration are linear with a zero intercept establishing that the initial reaction is first order in both $\text{FlH}_{2\text{T}}$ and ethyl pyruvate. Table II presents the rate constants (k_p) calculated from the initial burst by using the simple first-order analysis assuming an infinity extrapolated from the slower second phase of the reaction. From the dependence of the k_p constants upon $[\text{ethyl pyruvate}]$ the apparent second-order rate constant for reaction of ethyl pyruvate with $\text{FlH}_{2\text{T}}$ is $k_p = 1.25 \text{ M}^{-1} \text{ min}^{-1}$ (at pH 5.9). The rate of production of Fl_{ox} following the initial burst, k_s , is independent of the concentration of ethyl pyruvate (Table II) as expected from Scheme I. Finally the product analysis (Experimental Section) establishes that ethyl lactate is produced as the sole product from ethyl pyruvate.

Figure 7 depicts the variation of the absorbance-time course as the pH is varied for the reaction of pyruvamide (0.1 M) with $\text{FlH}_{2\text{T}}$ (7×10^{-5} M, $\mu = 1.0$, 30°C). The initial burst increases as the pH becomes more acidic and concomitantly the second

Table I. Rate Constants Evaluated Employing the Analog Computer Simulation Based on Scheme III for the Reaction of FlH_2 (7×10^{-5} M) with 0.1 M Carbonyl Substrate

Carbonyl substrate	pH	k_1 , $\text{M}^{-1} \text{min}^{-1}$	k_{-11} , min^{-1}	k_2 , min^{-1}	k_{-21} , min^{-1}	k_3 , $\text{M}^{-1} \text{min}^{-1}$	k_4 , $\text{M}^{-1} \text{min}^{-1}$	k_5 , min^{-1}	k_{-5} , $\text{M}^{-1} \text{min}^{-1}$
Ethyl pyruvate	5.90	8.20×10^{-1}	1.89×10^{-2}	4.94×10^{-2}	2.29×10^{-2}	1.00×10^{-1}	3.97×10^3	2.79×10^{-1}	40.6
	6.60	3.02	6.03×10^{-2}	1.06×10^{-1}	2.42×10^{-1}	1.51×10^{-1}	7.89×10^3	5.74×10^{-1}	92.8
Pyruvamide	7.20	2.74×10^{-1}	1.51×10^{-2}	1.34×10^{-2}	6.31×10^{-3}	2.76×10^{-2}	2.05×10^2	1.52×10^{-2}	217

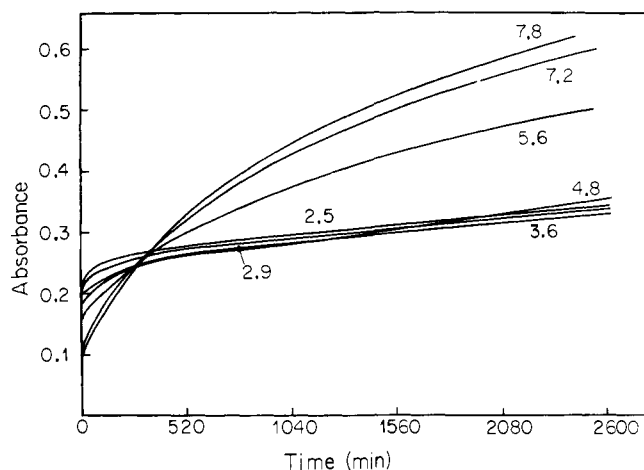


Figure 7. Absorbance vs. time plots for the reaction of pyruvamide (0.10 M) with 1,5-dihydroxymethylflavin-3-acetic acid (7.0×10^{-5} M) at 30°C , $\mu = 1.0$ with KCl, and 0.1 M buffer at various pH values. More acidic pH's show larger burst reactions and conversely more basic pH's show less burst and more rapid secondary reaction. All traces shown start at 0 absorbance.

following reaction is slowed. Conversely, the second phase becomes more facile as the pH becomes more basic. This behavior is also observed with other carbonyl substrates. Computer fits of the time courses for the reaction of FlH_{2T} with pyruvamide were not reliable beyond 50% production of Fl_{ox} . Figures 1C and 6D demonstrate the analog solution applied to the absorbance-time course of pyruvamide (0.1 M) with FlH_{2T} (7×10^{-5} M, $\mu = 1.0$, 30°C , pH 7.2, 0.1 M phosphate buffer). The fit is good for the portion of the reaction shown. However, the analog solution predicts continuing production of Fl_{ox} after ca. 23 h; whereas, from separate experiments in the absence of FlH_{2T} and at pH 7.0, it can be shown that all pyruvamide has disappeared from solution at ~ 23 h (due to its dimerization as followed at 343 nm). Table I lists the computer generated apparent rate constants for this one reaction at pH 7.2. No attempt has been made to obtain rate constants by fitting the other plots of Figure 7 to the computer program for Scheme II.

From the pH dependence of the calculated (see Discussion) ΔG° for the equilibrium $\text{FlH}_{2T} + \text{pyruvamide}_T \rightleftharpoons \text{Fl}_{\text{ox}} + \text{lactamide}_T$, it is apparent that the reaction should proceed in forward and reverse directions depending upon pH and the initial concentrations of pyruvamide and lactamide, respectively. Further, in the direction $\text{lactamide} + \text{Fl}_{\text{ox}} \rightarrow \text{pyruvamide} + \text{FlH}_{2T}$, the product pyruvamide is removed from solution by its self-condensation. At 0.1 M lactamide and 6×10^{-5} M Fl_{ox} the observed first-order rate constants for disappearance of Fl_{ox} were found to be $2.49 \times 10^{-2} \text{ min}^{-1}$ (pH 12.4) and $2.74 \times 10^{-3} \text{ min}^{-1}$ (pH 11.6) after correcting for the concurrent hydrolysis of Fl_{ox} . The hydrolytic rate for Fl_{ox} is $1.6 \times 10^{-3} \text{ min}^{-1}$ at pH 12.4 and $2.4 \times 10^{-4} \text{ min}^{-1}$ at pH 11.6. A product analysis for pyruvamide was not attempted due to the presence of Fl_{ox} hydrolytic products, the assured self-condensation of pyruvamide³² and the relatively high concentration of lactamide employed. In a following study, how-

Table II. Effect of the Concentration of Ethyl Pyruvate on $k_p = k_3 + k_1$, the Rate Constant for Partitioning Between the Direct Production of Fl_{ox} and 5-Carbinolamine and k_s (Calculated as an Apparent Zero-Order Constant), the Slow Secondary Production of Fl_{ox} (pH 5.90, $\mu = 1.0$, 30°C)

[Ethyl pyruvate], M	k_p , min^{-1}	k_s , M min^{-1}
0.055	0.039	1.13×10^{-7}
0.092	0.116	1.07×10^{-7}
0.100	0.127	1.10×10^{-7}
0.183	0.231	1.30×10^{-7}
0.275	0.358	1.27×10^{-7}
0.366	0.453	1.12×10^{-7}

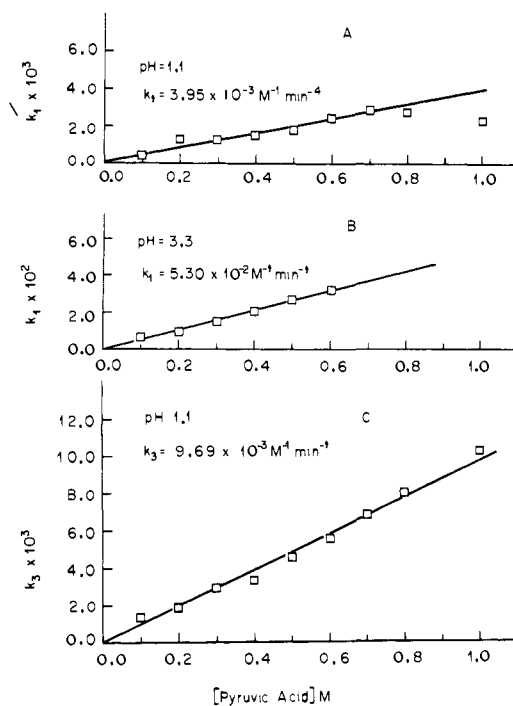


Figure 8. Dependence of k_1 and k_3 on the concentration of pyruvic acid when [1,5-dihydroxymethylflavin-3-acetic acid] = 7.0×10^{-5} M at 30°C , $\mu = 1.0$ with KCl.

ever, it is established that the co-product of reduction of Fl_{ox} by methanol is formaldehyde.²¹

Figures 1A and 1B exhibit the typical analog solutions for the reaction of pyruvic acid (0.1 M) with FlH_{2T} (7×10^{-5} M) at two widely separated pH's. As the pH becomes more acidic the initial burst ceases to be a distinct portion of the trace. Figures 6A and 6B show the computed time dependencies of the concentrations of all reactants, intermediates, and products according to Scheme III. The dependence of the various rate constants upon pyruvic acid concentration was determined by the computer fitting of the time courses for two pyruvic acid dilution experiments one above (pH 3.3) and the other below (pH 1.1) the pK_a of pyruvic acid (2.2).^{12,13} Nine pyruvate dilutions (0.1 to 1.0 M) were employed at pH 1.1 and seven (0.1 to 0.8 M) dilutions at pH 3.3. At pH 3.3 precipitation of sodium pyruvate occurred at 0.7 M and above. Only the k_1 and

Table III. Rate Constants Obtained from the Analog Simulation of Scheme III for the Reaction of FlH_2T with Pyruvic Acid at pH's Above and Below the pK_a of Pyruvic Acid^a

[Pyruvic acid] pH	$k_1 \times 10^3, \text{min}^{-1}$	$k_{-1} \times 10^3, \text{min}^{-1}$	$k_2 \times 10^3, \text{min}^{-1}$	$k_{-2} \times 10^4, \text{min}^{-1}$	$k_3 \times 10^3, \text{min}^{-1}$	$k_4 \times 10^{-2}, \text{M}^{-1} \text{min}^{-1}$	$k_5 \times 10^3, \text{M}^{-1} \text{min}^{-1}$	$k_{-5}, \text{M}^{-1} \text{min}^{-1}$	
0.1	1.10	0.395	4.31	9.34	8.68	1.36	1.34	9.02	0.295
0.2		1.32	1.64	7.13	7.98	1.82	1.32	8.84	0.303
0.3		1.35	2.09	9.28	8.46	2.98	1.47	8.98	0.356
0.4		1.49	2.04	9.04	8.67	3.37	1.30	8.72	0.284
0.5		1.85	2.34	9.39	8.55	4.60	1.80	12.1	0.415
0.6		2.45	1.94	10.9	8.56	5.59	1.83	12.3	0.421
0.7		2.87	1.76	9.23	8.50	6.85	1.52	9.45	0.402
0.8		2.82	1.99	9.03	8.64	7.92	1.39	8.85	0.394
1.0		2.35	3.50	8.88	8.43	10.2	1.28	8.10	0.314
Av			2.4 ± 0.9	9.36 ± 0.6	8.50 ± 0.2		1.47 ± 0.2	9.60 ± 1.5	0.359 ± 0.06
		$k_1 \times 10^2$	$k_{-1} \times 10^2$	$k_2 \times 10^2$	$k_{-2} \times 10^2$	$k_3 \times 10^3$	$k_4 \times 10^{-2}$	$k_5 \times 10^{-2}$	k_{-5}
0.1	3.30	0.624	5.33	2.29	2.00	1.10	6.98	5.32	1.98
0.2		0.917	4.64	2.17	2.12	2.68	5.53	4.26	1.53
0.3		1.51	5.81	2.08	2.21	5.16	7.24	5.43	2.11
0.4		2.02	5.46	2.19	2.11	7.71	7.66	5.61	2.16
0.5		2.71	5.34	2.08	2.05	12.2	7.54	5.54	2.08
0.6		3.25	5.71	2.12	2.15	21.0	7.66	5.61	2.27
Av			5.38 ± 0.4	2.16 ± 0.1	2.11 ± 0.1		7.10 ± 0.8	5.30 ± 0.5	2.02 ± 0.3

^a [Pyruvic acid] was varied, and the average values for the concentration independent steps are given with their corresponding standard deviation.

Table IV. Rate Constants k_5 and k_{-5} Generated from Analog Simulation of Scheme III for the Reaction of Pyruvic Acid (0.1 M) with FlH_2T (7×10^{-5} M) at Varying pH Values

pH	k_5, min^{-1}	$k_{-5}, \text{M}^{-1} \text{min}^{-1}$
0.07	9.13×10^{-4}	0.357
0.07	9.20×10^{-4}	0.357
0.13	1.13×10^{-3}	0.841
0.15	9.62×10^{-4}	0.373
0.46	1.25×10^{-2}	0.357
0.53	1.36×10^{-3}	0.962
0.79	9.20×10^{-4}	0.527
0.86	1.05×10^{-3}	0.411
0.89	6.22×10^{-3}	0.342
1.07	9.26×10^{-3}	0.276
1.10	9.02×10^{-3}	0.295
1.52	8.22×10^{-3}	0.334
1.90	2.01×10^{-2}	0.411
1.91	1.06×10^{-2}	0.810
1.93	1.11×10^{-2}	0.922
2.02	3.02×10^{-2}	1.49
2.09	2.45×10^{-2}	1.73
2.13	2.44×10^{-2}	1.68
2.32	3.14×10^{-2}	1.62
2.83	1.78×10^{-2}	1.08
2.88	1.02×10^{-2}	0.944
3.27	3.44×10^{-2}	1.45
3.33	4.26×10^{-2}	1.53
3.86	6.32×10^{-2}	1.80
4.05	3.42×10^{-2}	1.52
4.69	5.24×10^{-2}	1.72
4.89	1.34×10^{-1}	1.73
5.74	2.68×10^{-1}	1.73

k_3 steps of Scheme I should be pyruvic acid dependent, and this expectation is supported by the analog solution for the pyruvate dilution experiments. Figures 8A and 8B present plots of k_1 (Scheme I) vs. [pyruvic acid] at pH's 1.1 and 3.3. The plots are linear establishing a first-order dependence of k_1 on [pyruvate]. The second-order rate constants, obtained from the slopes of the lines are $3.95 \times 10^{-3} \text{ M}^{-1} \text{ min}^{-1}$ at pH 1.1 and $5.30 \times 10^{-2} \text{ M}^{-1}$ at pH 3.3. A similar pyruvic acid concentration dependence is obtained (Figure 8C) for the observed k_3 step at pH 1.1 allowing calculation of a second-order rate constant of $9.69 \times 10^{-3} \text{ M}^{-1} \text{ s}^{-1}$. However, at pH 3.3 the dependence of k_3 on pyruvic acid becomes nonlinear as evidenced by Figure 9A. A second-order dependence upon pyruvic acid is shown

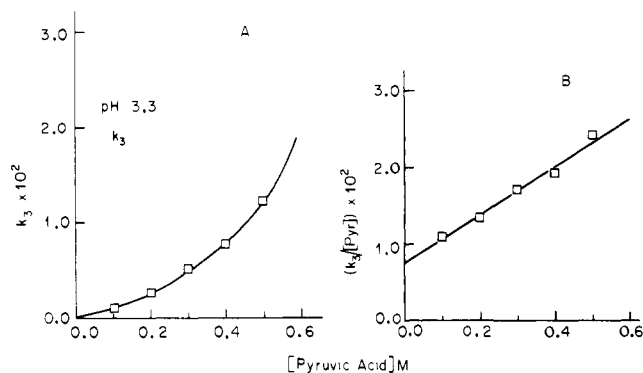


Figure 9. Dependence of k_3 on the concentration of pyruvic acid at pH 3.3 when [1,5-dihydroflavin-3-acetic acid] = 7.0×10^{-5} M at 30°C and $\mu = 1.0$ with KCl.

in Figure 9B where $k_3/[\text{pyruvic acid}]$ is plotted vs. [pyruvic acid]. From the intercept of the plot ($[\text{pyruvic acid}] = 0$), there is obtained the apparent first-order dependence on pyruvic acid ($k_3' = 7.30 \times 10^{-3} \text{ M}^{-1} \text{ min}^{-1}$) and from the slope the apparent second-order dependence on [pyruvic acid] ($k_3'' = 3.20 \times 10^{-2} \text{ M}^{-2} \text{ min}^{-1}$). The remaining rate constants derived from the analog solutions were, as expected, independent of [pyruvic acid]. Table III lists the individual constants of Scheme III at the various pyruvate concentrations and at pH's 1.1 and 3.3.

The pH dependence of the reaction of pyruvic acid (0.1 M) with FlH_2T (7×10^{-5} M) was determined over the pH range of 0 to 6. The computed values of k_{-5} and k_5 are listed in Table IV and $\log k_{\text{rate}}$ vs. pH profiles for k_1 , k_{-1} , k_2 , k_{-2} , k_3 , and k_4 are plotted in Figures 10A-F, respectively. At 0.1 M pyruvic acid the contribution of k_3'' and k_3' are almost equivalent so that the plot of $\log k_{\text{obsd}}$ vs. k_3 (Figure 10E) may be employed to determine the pH dependence of k_3' .

Discussion

It has been suggested that the dihydroflavin ($\text{FlH}_2 + \text{FlH}^-$) reduction of carbonyl compounds can occur through either a $1e^- + \text{H}^+$, a $1e^- + 1e^- + \text{H}^+$ reaction, or both depending upon the acidity of the C-H bond of the resultant H-C-OH moi-

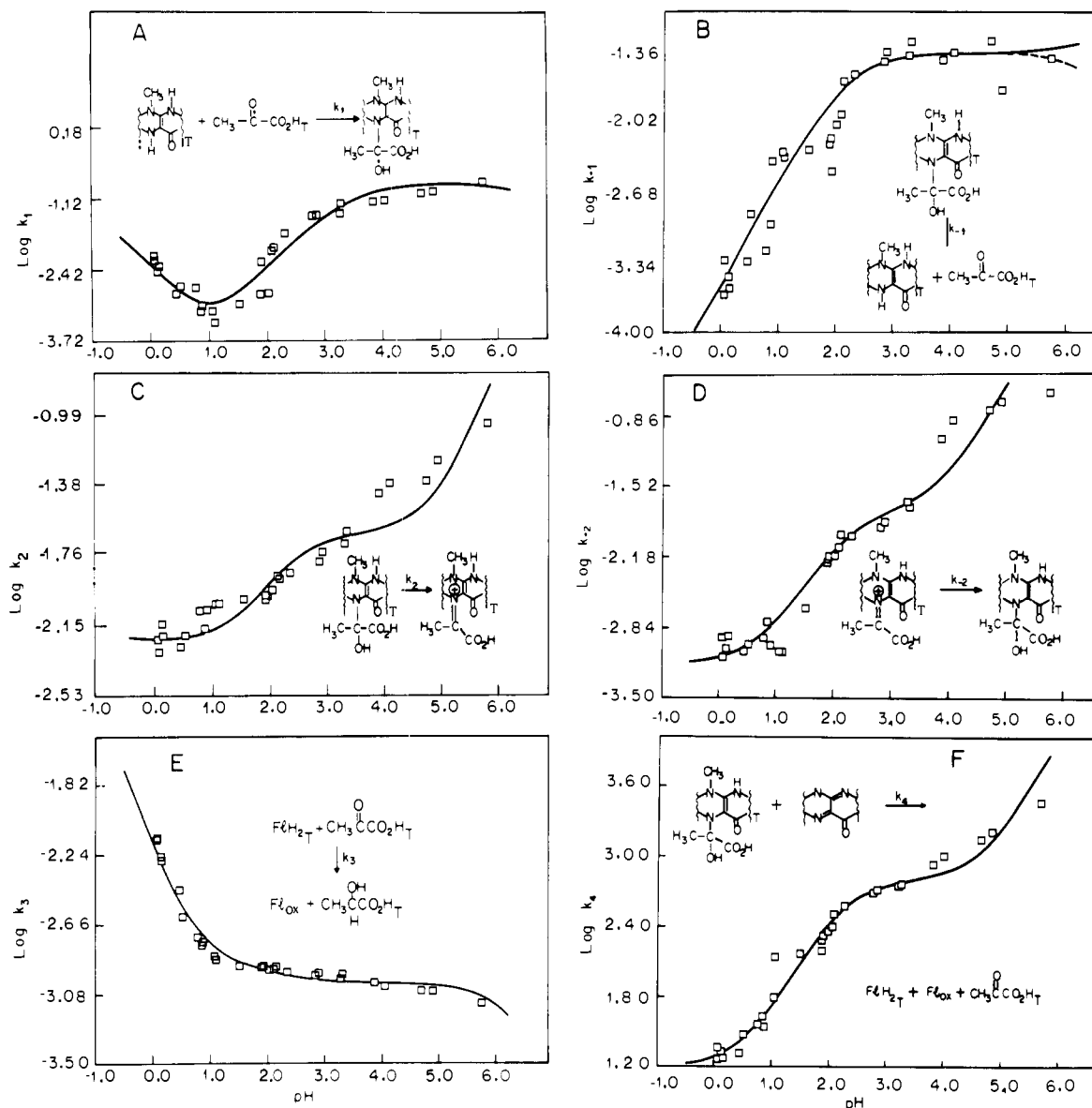


Figure 10. Log k_{rate} vs. pH profile for the rate constants derived from the analog solution of Scheme II for the reaction of pyruvic acid (0.10 M) with [1,5-dihydroxylumiflavin-3-acetic acid] = 7.0×10^{-5} M.

ety.^{2,4} Part 1³ has established that $1e^-$ transfer from *N*(5)-alkyl-1,5-dihydroflavins to carbonyl compounds to provide the *N*(5)-alkylflavinium cation radical occurs when the difference in potentials of oxidant and reductant were sufficiently great. The primary purpose of the present investigation and the following papers of this series has been threefold: (1) to establish if, as suggested by others,¹⁹ the dihydroflavin derived carbinolamines and imines are involved as intermediates in the dihydroflavin reduction of carbonyl substrates; (2) to evaluate the overall kinetic scheme for reaction of dihydroflavins with carbonyl substrates; and (3) to determine if radical intermediates are thermodynamically allowed in the reduction process. Employing ethyl pyruvate, pyruvamide, and pyruvic acid (aqueous solution in the pH range from 0–9), both 5-carbinolamine ($\lambda_{\text{max}} \sim 350$ nm) and the corresponding imine ($\lambda_{\text{max}} \sim 500$) are observed and the imine may be trapped with NaCNBH_3 . The product of NaCNBH_3 trapping is an *N*(5)-alkyl-1,5-dihydroflavin (obtained even at pH 7 with pyruvate where essentially no reduction of pyruvate by FlH_{2T} occurs), and this may be assayed by $^3\text{O}_2$ oxidation to the relatively stable flavin aminium cation radical (Experimental Section). Therefore, there is no doubt that a *N*(5) adduct forms on reaction of a carbonyl compound with a dihydroflavin. However,

the spectral buildup of the 5-carbinolamine and derived imine species is concomitant with a decrease in Fl_{ox} production (initial burst). The reactions of Scheme I have now been established for pyruvic acid, pyruvamide, and ethyl pyruvate. The production of Fl_{ox} in an "initial burst" is dependent upon the partitioning of FlH_{2T} between carbinolamine (k_1) and Fl_{ox} (k_3). The percent conversion of initial FlH_{2T} to Fl_{ox} , when NaCNBH_3 is present at the beginning of the reaction, is quantitatively coincident with that expected from the ratio of k_1 to k_3 obtained from the analog solutions of the time dependence of Fl_{ox} production according to Scheme II (Results). Since trapping of the imines by NaCNBH_3 is very rapid and $k_2 > k_{-1}$ then the Fl_{ox} produced must come from a direct reaction (k_3 step). Clearly, the 5-carbinolamine and imine species are not on the reaction pathway but exist as products of a nonproductive equilibria.

Because of unwanted side reactions, ethyl pyruvate (hydrolysis) and pyruvamide (condensation) have received only cursory examination in their reaction with FlH_{2T} . Nonetheless, these studies are sufficient to establish that both substrates are reduced by FlH_{2T} , and in the case of ethyl pyruvate it has been shown that ethyl lactate and Fl_{ox} are the only products. The oxidation-reduction reaction (reaction b of Scheme II) has

been shown to be first order in $\text{FlH}_{2\text{T}}$ and ethyl pyruvate or pyruvamide, respectively. The kinetic data and derived constants for these substrates are contained in the Results section. The reaction of pyruvic acid and pyruvate with FlH_2 plus FlH^- has been more extensively investigated. The pH and [pyruvate + pyruvic acid] dependence of the rate constants of Scheme II has been determined (Table III and Figure 10A–F). The values of k_5 and k_{-5} (Table IV) show very little or no pH dependence. Since the pH dependence for the comproportionation of an $N(5)$ -alkyldihydroflavin with oxidized flavin is yet to be investigated, there is no basis for judging the reasonableness of this finding. Although it has been established that Fl_{ox} does not produce an observable amount of $N(5)$ -alkyl radical when it is reacted with either the $N(5)$ -methyl- or $N(5)$ -ethyl-1,5-dihydroflavin,^{20a} it has been shown to enter into complexation with the $N(5)$ -alkyl reduced species.²⁰ The carbinolamine-imine moiety on the $N(5)$ position would be expected to facilitate electron transfer and subsequent radical formation. As the analog solutions show (Figure 6A–D), radical complex (indicated CT) does not accumulate to any extent. Electron transfer may occur with loss of the aldehyde moiety of the carbinolamine. No further comment upon the comproportionation step is allowed. Log k_{rate} vs. pH profiles have been constructed for the remaining rate constants at a value of [pyruvic acid + pyruvate] = 0.10 M. These are presented in Figure 10A–F. What remains is a discussion of the reasonableness of the profiles for the forward and reverse reactions attributed to carbinolamine and imine formation and, most importantly, the mechanistic evaluation of the log k_3 vs. pH profile for direct reduction of pyruvic acid and pyruvate by dihydroflavin.

The log k_{rate} vs. pH profiles of Figures 10A to 10F have been fitted via the rate expressions of eq 5 to 10:

$$k_1 = \frac{k_{1a}a_{\text{H}}^3 + k_{1b}a_{\text{H}}}{(a_{\text{H}} + K_{a1})(a_{\text{H}} + K_{a2})} \quad (5)$$

or

$$k_1 = \frac{k_{1a}a_{\text{H}}^3 + k_{1b}a_{\text{H}}^2 + k_{1c}a_{\text{H}}}{(a_{\text{H}} + K_{a1})(a_{\text{H}} + K_{a2})}$$

$$k_{-1} = \frac{k_{-1a}a_{\text{H}}^2 + k_{-1b}a_{\text{H}} + k_{-1c}}{a_{\text{H}}^2 + a_{\text{H}}K_{a1} + K_{a1}K_{a2}} \quad (6)$$

or

$$k_{-1} = (k_{-1a}a_{\text{H}}^2 + k_{-1b}a_{\text{H}})/(a_{\text{H}}^2 + a_{\text{H}}K_{a1} + K_{a1}K_{a2})$$

$$k_2 = \frac{k_{2a}a_{\text{H}}^3 + k_{2b}a_{\text{H}}^2 + k_{2c}a_{\text{H}} + k_{2d}}{a_{\text{H}}^2 + a_{\text{H}}K_{a1} + K_{a1}K_{a2}} \quad (7)$$

$$k_{-2} = \frac{k_{-2a}a_{\text{H}}^2 + k_{-2b}a_{\text{H}} + k_{-2c} + k_{-2d}/a_{\text{H}}}{a_{\text{H}}^2 + a_{\text{H}}K_{a1} + K_{a1}K_{a2}} \quad (8)$$

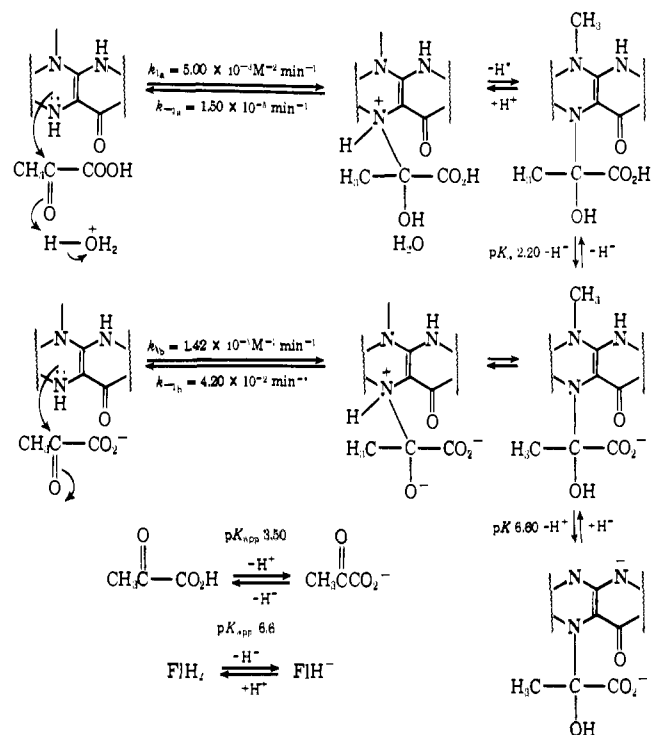
$$k_3 = \frac{k_{3a}a_{\text{H}}^3 + k_{3b}a_{\text{H}}^2 + k_{3c}a_{\text{H}}}{(a_{\text{H}} + K_{a1})(a_{\text{H}} + K_{a2})} \quad (9)$$

$$k_4 = \frac{k_{4a}a_{\text{H}}^2 + k_{4b}a_{\text{H}} + k_{4c}}{a_{\text{H}}^2 + a_{\text{H}}K_{a1} + K_{a1}K_{a2}} \quad (10)$$

The kinetic expressions of eq 5 to 10 are in accord with the mechanisms of Schemes III to VI.

Though Scheme III represents the simplest reaction sequence which allows a fit of the pH dependence of carbinolamine formation, it is not unique. The log k_1 vs. pH plot of Figure 10A may be duplicated by employing the reaction sequence of Scheme VII. The order of the rate constants for either scheme is reasonable and the pH–log k_1 profile (Figure 10A) is of a form not unexpected for carbinolamine formation involving a weakly basic amine (see examples in ref 23, 34). The equilibrium constant for carbinolamine formation, k_1/k_{-1} , is 3.3 M^{-1} at pH 2 when the rate constants of either Scheme

Scheme III. Carbinolamine Formation

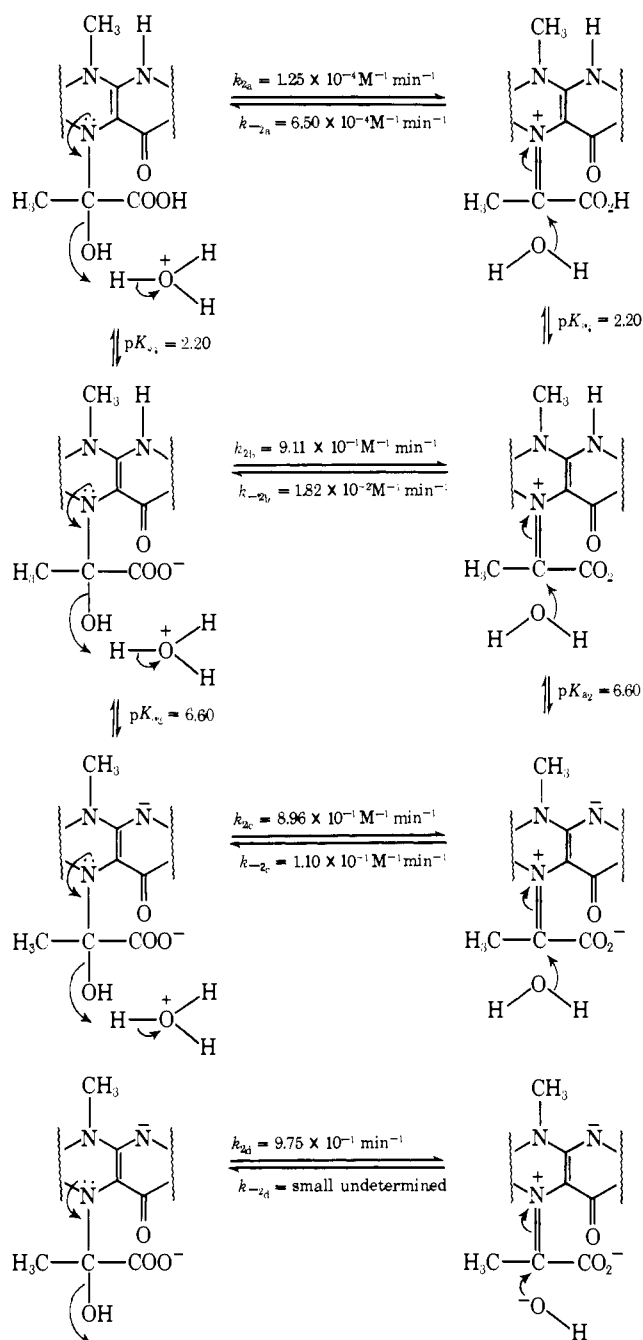


III or VII are used in the calculation. Applying a correction for the amount of hydrated pyruvic acid ($K_{\text{Hyd}} = [\text{hydrate}]/[\text{pyruvic acid}] = 0.7$ at pH 2)¹² gives $k_1/k_{-1} = 5.7 \text{ M}^{-1}$. The $N(5)$ position of the flavin is very weakly basic. The equilibrium constant for carbinolamine formation between pyridine-4-carboxaldehyde and urea, a very weak base, is $K_{\text{CA}} = 1.3$.^{34d} Several other amines show equilibrium constants of the same order of magnitude^{34d} as observed for the carbinolamine formation between 1,5-dihydroflavin and pyruvic acid. Of the four reaction steps for interconversion of carbinolamine and imine (Scheme IV) the second and fourth are kinetically equivalent. According to Scheme IV, the greater the electron delocalization to the (+)N(5) position, the more favorable the equilibrium constant for imine formation ($k_2/k_{-2} = 0.19$, 50, 8150). This is due primarily to the greater driving force for the forward dehydration steps ($k_{2a}:k_{2b}:k_{2c} = 1:7.3 \times 10^3:7.2 \times 10^8$). The equilibrium constants for imine formation of several substituted *p*-chlorobenzaldehyde hydrazones lie between 10^4 and 10^5 (*p*-toluenesulfonylhydrazide: $K_{\text{CA}} = 1.7$, $K_{\text{IM}} = 1.4 \times 10^4$).^{23a} The rate of hydration of imine is actually decreased by the same electronic effects, this being due, no doubt, to greater electron release to the (+)N(5) position ($k_{-2a}:k_{-2b}:k_{-2c} = 1:28:1.69 \times 10^4$). The overall result is a lowering of the ΔG^\ddagger barriers in going from the reactions of k_{2a}/k_{-2a} to k_{2c}/k_{-2c} . Rate constants for the oxidation of carbinolamine species by Fl_{ox} (Scheme V) are in the order anticipated. Thus, the greater the electron density of the carbinolamine the more facile the electron-transfer reaction (i.e., $k_{4a}:k_{4b}:k_{4c} = 1:38:2445$).

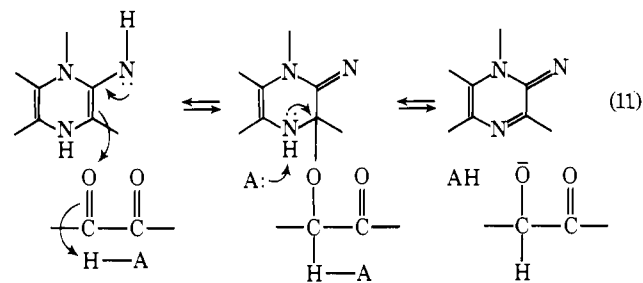
The reaction of primary concern to this study involves the reduction of pyruvic acid and pyruvate to lactic acid by dihydroflavin (Scheme VI). Three terms are required to fit the pH–log k_3 profile (Figure 10E), and these are k_{3a} , k_{3b} , and k_{3c} . The reaction associated with k_{3a} is unambiguously hydronium ion catalyzed reduction of pyruvic acid by undissociated 1,5-dihydroflavin. In the case of k_{3b} and k_{3c} , choices are allowed between three kinetically equivalent mechanisms (see Scheme VI).

Mechanisms involving $2e^-$ transfer via covalent intermediates have been proposed to be ubiquitous for flavin oxidation and reduction of organic substrates.^{35–37} The proposal of

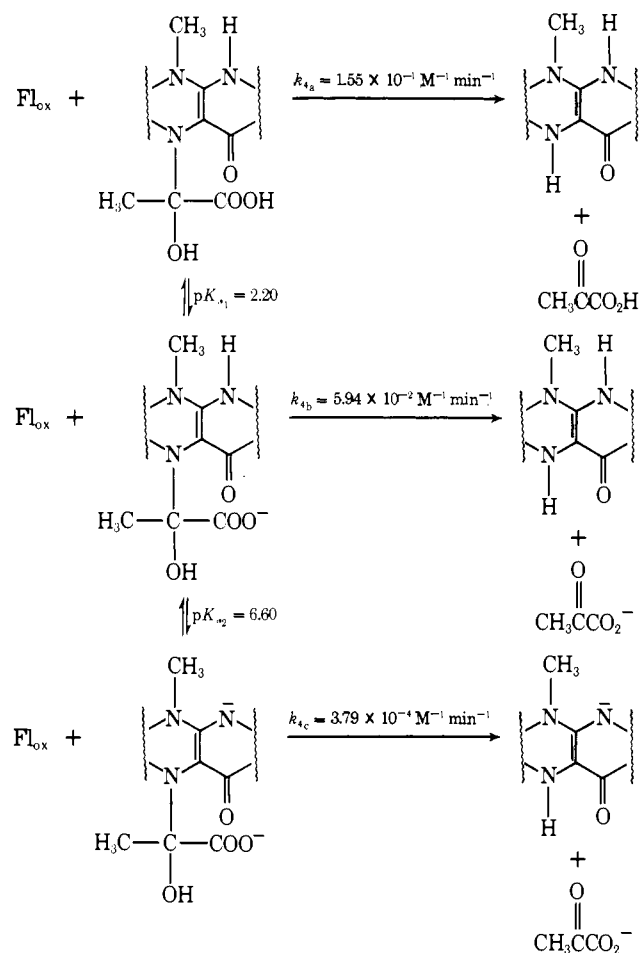
Scheme IV. Imine Formation



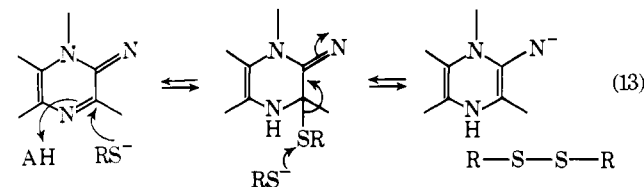
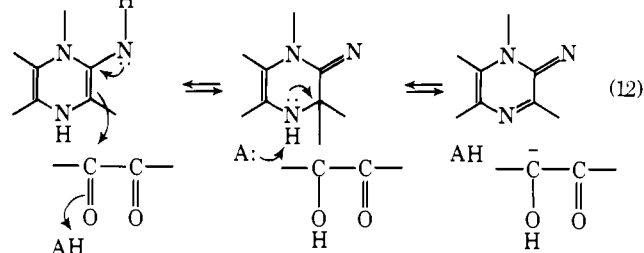
Blankenhorn, Ghisla, and Hemmerich¹⁹ that the 5-carbinolamine is an intermediate in carbonyl group reduction is obviously not correct. Brown and Hamilton³⁶ have suggested the 4a-mechanism of eq 11 to which may be added the mechanism



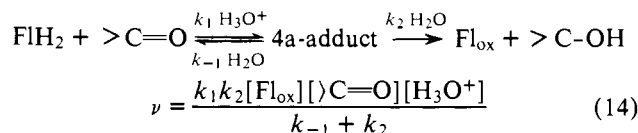
of eq 12.⁴ A 4a-addition-elimination reaction has been established for the oxidation of thiols by Fl_{ox} (eq 13).³⁸ General acid protonation of the N(5) position accompanying nucleo-

Scheme V. Oxidation of Carbinolamine by Fl_{ox}

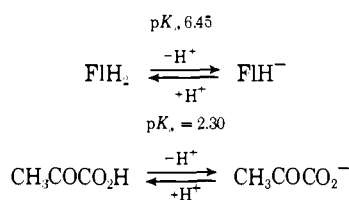
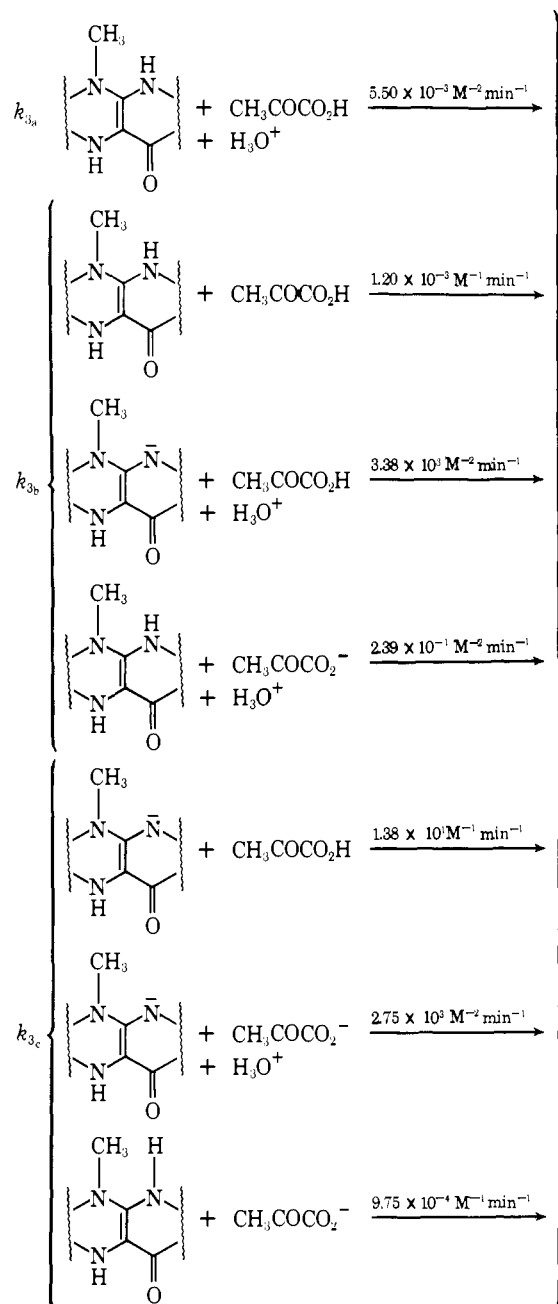
philic attack at the 4a-position is anticipated (eq 11 and 12). This feature has been established for oxidation of thiols by Fl_{ox}³⁸ and for addition of SO₃²⁻ to the 4a-position.³⁹ From Figure 9 it may be seen that the reduction of pyruvic acid is catalyzed by pyruvic acid.



Since there appears to be no spectral or kinetic requirement for an intermediate in the reduction of pyruvate by dihydroflavin, the correctness of the mechanisms of either eq 11 or 12 requires that the respective 4a-adduct be at steady state:

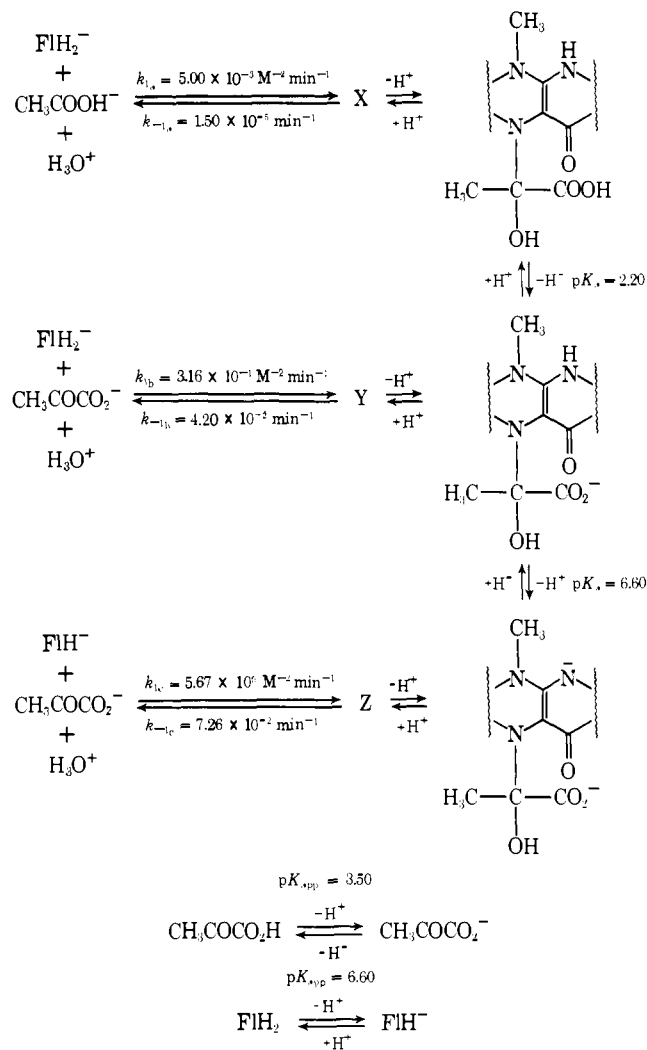


Scheme VI. Reduction of Pyruvate by Dihydroflavin

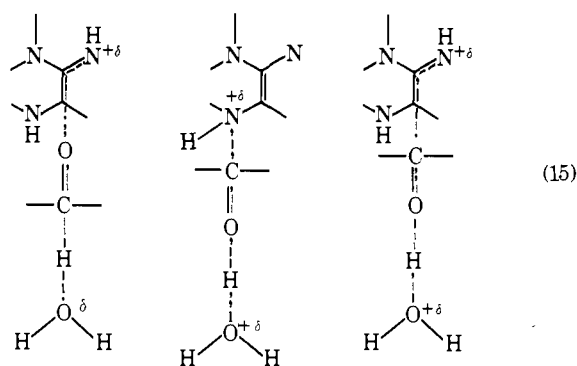


On this basis, the mechanism of eq 11 may be dismissed. Thus, the formation of carbinolamine is competitive with the direct reduction of carbonyl compound. Comparison of the rate constants for H_3O^+ -catalyzed carbinolamine and reduction of carbonyl compound (i.e., k_{1a}/k_{3a}) reveals that they are essentially equal. For the mechanism of eq 11 to be correct it is required that acid-catalyzed enamine attack upon carbonyl oxygen be as facile as acid-catalyzed attack of the N(5) nitrogen upon carbonyl carbon (eq 15). The mechanism of eq 12 may not be dismissed on this basis since enamine attack upon carbonyl carbon might well be competitive with carbinolamine formation. In addition, as shown in the following study,²⁷ the

Scheme VII. Alternate Scheme for Carbinolamine Formation



carbanion rather than the alkoxide ion is the direct substrate for the Fl_{ox} oxidation of benzoin to benzil. This feature would be in accord with the mechanism of eq 12 but clearly not with that of eq 11.



An alternative to the $2e^-$ reduction of pyruvate via the formation of a 4a-adduct (eq 14) is a mechanism involving the

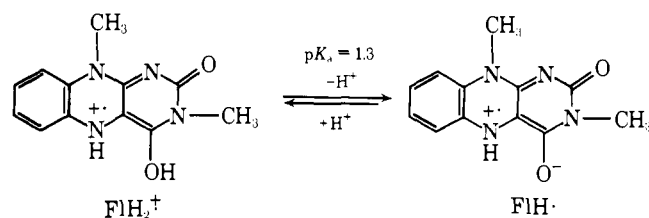
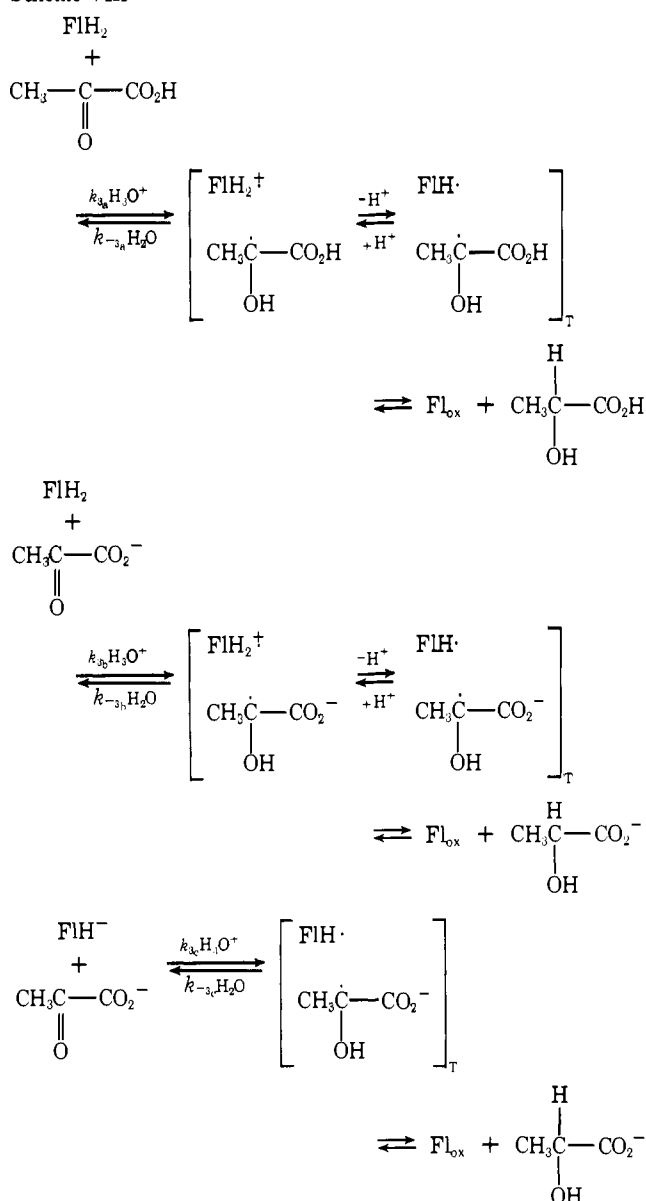


Table V. ΔE_m Values and Corresponding ΔG° for the Potential Difference Between Lactate/Pyruvate and Dihydroflavin/Oxidized Flavin Couples

pH	E_m		ΔE_m	$\Delta G^\circ{}^a$
	$\text{CH}_3\text{CH}(\text{OH})\text{COOH}_T/\text{CH}_3\text{C}(=\text{O})\text{COOH}_T$	$\text{FlH}_2T/\text{Fl}_{\text{ox}}$		
0	+0.224 ^b (+0.253) ^c	+0.201	-0.023 ^b (-0.052) ^c	-1.06 ^b (-2.40) ^c
1	+0.162 (+0.191)	+0.140	-0.022 (-0.051)	-1.02 (-2.35)
2	+0.095 (+0.124)	+0.079	-0.016 (-0.045)	-0.74 (-2.08)
3	+0.016 (+0.045)	+0.018	+0.002 (-0.027)	+0.09 (-1.24)
4	-0.064 (-0.035)	-0.043	+0.021 (-0.008)	+0.97 (-0.37)
5	-0.132 (-0.103)	-0.104	+0.028 (-0.001)	+1.29 (-0.05)
6	-0.193 (-0.164)	-0.160	+0.033 (+0.004)	+1.52 (+0.18)
7	-0.255 (-0.226)	-0.202	+0.053 (+0.024)	+2.44 (+1.11)
8	-0.316 (-0.287)	-0.235	+0.081 (+0.052)	+3.74 (+2.40)
9	-0.377 (-0.348)	-0.266	+0.111 (+0.082)	+5.12 (+3.78)
10	-0.438 (-0.409)	-0.305	+0.133 (+0.104)	+6.13 (+4.80)
11	-0.499 (-0.470)	-0.358	+0.141 (+0.112)	+6.50 (+5.17)
12	-0.560 (-0.531)	-0.418	+0.142 (+0.113)	+6.55 (+5.21)
13	-0.622 (-0.593)	-0.479	+0.143 (+0.114)	+6.60 (+5.26)

^a ΔG° represents the free energy difference between the initial and final ground states. ^b Values obtained from an E_0 determined from thermodynamic calculations by Burton.⁴⁵ ^c Values obtained from E_0 determined to be the best measured value by Clark.⁴⁰ ^d $\text{CH}_3\text{CH}(\text{OH})\text{COOH}_T/\text{CH}_3\text{C}(=\text{O})\text{COOH}_T$.

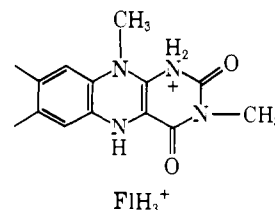
Scheme VIII



radical species $\text{FlH}_2^{\cdot+}$ and FlH^{\cdot} . In Scheme VIII the redox reactions are envisioned to occur by way of general acid cata-

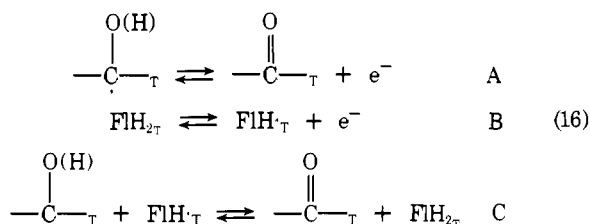
lyzed $1e^-$ transfer from dihydroflavin species to pyruvic acid or pyruvate to form radical pairs which go on to form product via H^{\cdot} or a second $1e^-$ transfer reaction from flavin radical to $\cdot\text{C}-\text{OH}$. Suggestive spectral evidence for the intermediacy of the flavin radical species during the direct reduction of pyruvic acid (Scheme VIII) is observed at 515 nm (inset, Figure 3). However, although the comproportionation reaction between Fl_{ox} and FlH_2T to produce $\text{FlH}T$ is probably slow at acidic pH,^{20b} it is not possible to completely rule out this possibility for production of the transient absorbance observed.

Assuming a relationship between ΔG° and ΔG^\ddagger , the ratio of the rate constants for dihydroflavin reduction of pyruvate + pyruvic acid are not unreasonable [i.e., $(\text{FlH}_2 + \text{PyrH} + \text{H}_3\text{O}^+):(\text{FlH}_2 + \text{Pyr}^- + \text{H}_3\text{O}^+):(\text{FlH}^- + \text{Pyr}^- + \text{H}_3\text{O}^+) = 1:43:5 \times 10^5$], as can be seen from electrochemical data. Thus, the maximal tenfold change in k_3 (Figure 3) with pH is in accord with expectations based on the differences in the midpoint potentials (ΔE_m) of the couples pyruvate/lactate⁴⁰ and dihydroflavin/oxidized flavin⁴¹ (Table V). Examination of Table V reveals that the value of ΔE_m is positive and virtually invariant between pH 3.5–6.0. From Figure 10E it may be seen that $\log k_3$ is virtually constant in this pH range. The ΔE_m becomes more positive above 6.0. At pH's >7.0, ΔE_m indicates that the reduction of pyruvate by FlH^- is thermodynamically unfavorable. As indicated (Results), lactate acts as a reducing agent for Fl_{ox} at high pH. At pH values less than 3.5 the value of ΔE_m decreases steadily until a plateau is reached at pH values below 1.3. This plateau arises due to the formation of FlH_3^+ . A calculation based on ΔE_m , assuming a relationship

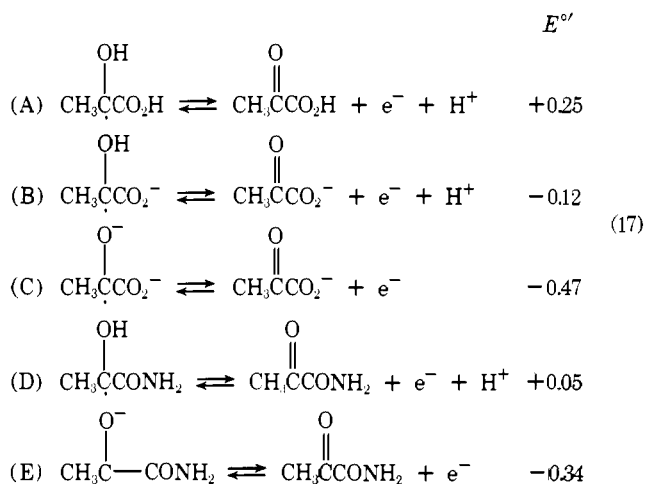


between ΔG° and ΔG^\ddagger , indicates that k_3 should exhibit a maximal change of ca. tenfold, as observed between pH 0 and 3.

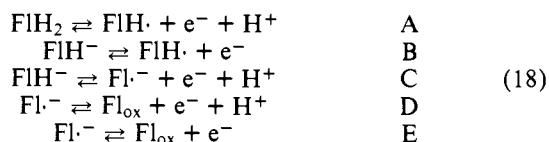
Sufficient electrochemical data exist to assess the reasonableness of radical pathways for the dihydroflavin reduction of the carbonyl compounds of this study. The computations which will be offered are based on the potential difference between the half-cell reactions of eq 16A and 16B which de-



termine the potential of 16C (where $\text{FlH}_{2\text{T}} \rightleftharpoons \text{FlH}_{2\text{a}} + \text{FlH}^-\text{b}$, a and b being mole fraction of FlH_2 and FlH^- , respectively, at a given pH). All computations have been carried out for the standard state of 1 M reactants, intermediates, and products, but at stipulated pH values. Thus, no corrections have been estimated or applied to the calculated free-energy levels for what are proposed to be solvent caged free radical pair intermediates. For this reason allowances for any stabilization by cage effects, charge transfer interactions, etc. have not been made and consequently, the calculated ΔG° levels are probably maximized. However, the potentials of Rao and Hayon (eq 17,



where E_0' represents the potential of the reaction at 7)⁴² have been employed. These E_0' values do not truly represent E° values but are kinetic potentials,⁴³ and this feature undoubtedly minimizes (by perhaps 5 kcal M^{-1}) the computed ΔG° values of formation of the radical intermediates. These two features should tend to cancel any errors in the computed standard free energies of formation. In any event, the computed energy levels could be in error by up to 10 kcal M^{-1} without altering our conclusions! The E_m values for the $1e^-$ half-cell reactions of eq 17A, 17B, and 17E were corrected to the appropriate pH (Nernst equation at 30 °C stipulates (-) 60.15 mV for each pH unit below 7 or (+) 60.15 mV for each pH above 7.0). Application of the pH correction provides Table VI. The five dihydroflavin half-cell reactions of eq 18 are required. Draper and Ingraham⁴¹ have presented a comprehensive study of the pH behavior of the midpoint potentials for the semiquinone/oxidized flavin and reduced flavin/semiquinone couples. In their study riboflavin was employed. Since small structural changes in the flavin moiety do not alter the determined E_0' values (i.e., $2e^-$ conversion of $\text{FlH}_{2\text{T}} \rightarrow \text{Fl}_{\text{ox}}$) for a variety of flavins (riboflavin; $E_0' = -0.201 \text{ V}^{42}$ and lumiflavin; $E_0' = -0.233 \text{ V}^{44}$), the E_0' values which are employed in these calculations have been interpolated from their data.

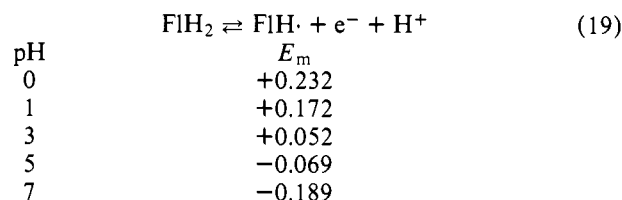


For the half-cell reaction of eq 19A the species FlH_2 and $\text{FlH}\cdot$ exhibit no ionic equilibria at low pH. Thus, the experi-

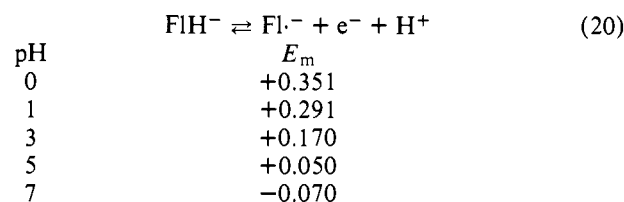
Table VI.

pH	E_m values		
	$\begin{array}{c} \text{OH} \\ \\ \text{CH}_3\text{C}\cdot\text{CO}_2\text{H} \end{array}$	$\begin{array}{c} \text{OH} \\ \\ \text{CH}_3\text{C}\cdot\text{CO}_2^- \end{array}$	$\begin{array}{c} \text{OH} \\ \\ \text{CH}_3\text{C}\cdot\text{CONH}_2 \end{array}$
0	+0.67	+0.30	+0.48
1	+0.61	+0.24	+0.42
3	+0.49	+0.12	+0.30
5	+0.37	+0.00	+0.18
7	+0.25	-0.12	+0.006

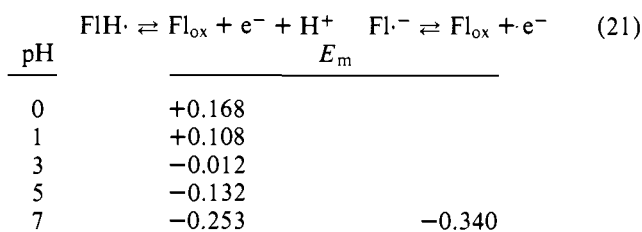
mental E_m values of Draper and Ingraham for the reduced flavin semiquinone couple⁴¹ may be employed to interpolate the required E_m values for 18A at desired pH values (eq 19):



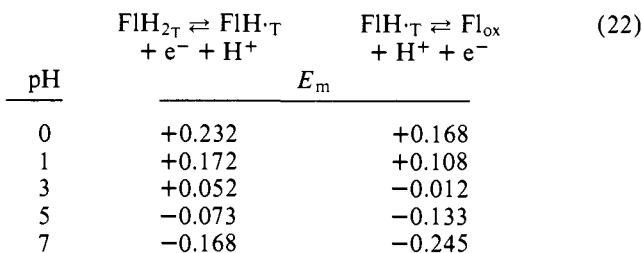
The E_m values for eq 18B at low pH may be obtained by applying a pH correction to the values determined by Draper and Ingraham above pH 10⁴¹ to give eq 20:



In a similar manner the E_m values for the half-cell reactions of eq 18D and 18E can be obtained from the semiquinone-oxidized flavin couple (eq 21):



Having determined the individual potential values of eq 18, it is necessary to compute the potentials at a given pH where all pertinent ionic species are taken into account. Conversion of the potentials to their corresponding free energies [$\Delta G = nFE$; $\Delta G = (E_m + 60.15 \text{ pH})/0.04336$], correction of each free energy based upon the contribution of the mole fraction of each species at the pH under consideration, and reconversion to E_m provides eq 22:



The E_m values of the half-cell reactions for pyruvic acid or pyruvamide were added to the E_m values of the flavin half-cell

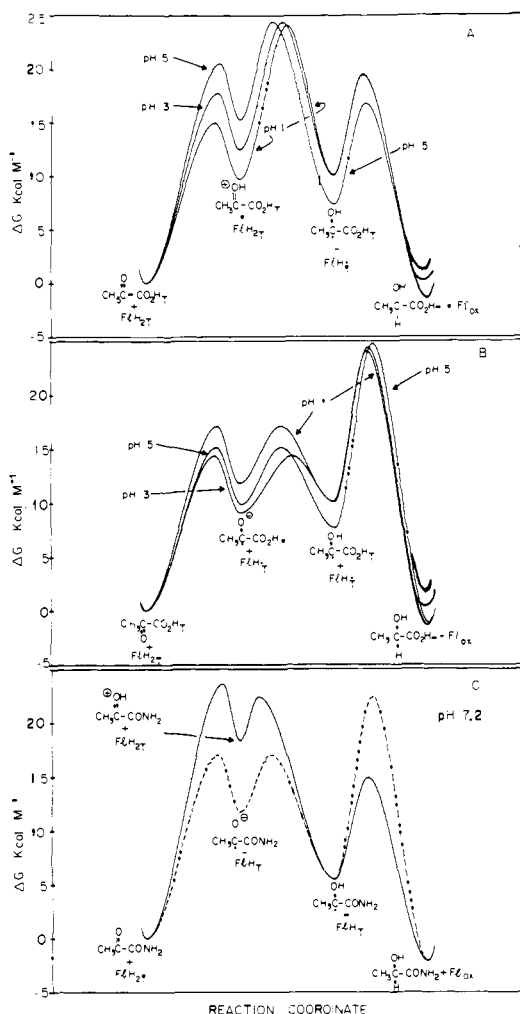
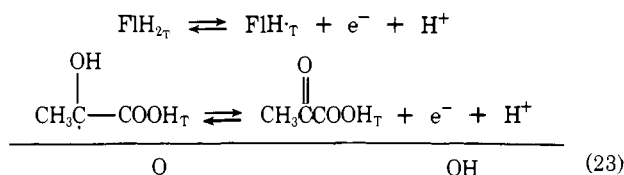


Figure 11. Reaction coordinate diagrams for the reaction of pyruvic acid and pyruvamide with 1,5-dihydroflavin-3-acetic acid under standard conditions of 1 M, 30 °C. The highest free energy barrier corresponds to the observed $\Delta G^\ddagger_{\text{exp}}$.

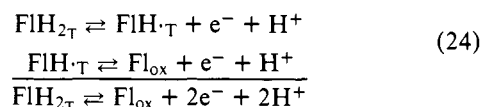
reactions to give a resultant ΔE_m expressed as a standard free energy for formation of the "radical pair" moieties at 1 M ($\Delta G^\circ = \Delta E_m$ 23.0603 at 30° for a $1e^-$ process as shown in eq 23 for pyruvic acid). In a like manner, the free-energy levels



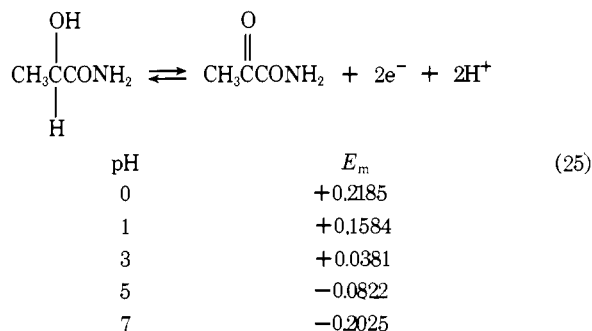
pH	ΔE_m	ΔG°
0	-0.439	10.12
1	-0.439	10.12
3	-0.437	10.07
5	-0.320	7.37

for $\text{CH}_3\dot{\text{C}}(\text{OH})\text{CONH}_2$ and $\text{CH}_3\dot{\text{C}}(\text{O}^-)\text{CONH}_2$ were determined. Since no experimental data are available for the species $\text{CH}_3\dot{\text{C}}(\text{O}^-)\text{CO}_2\text{H}$ the potentials obtained for the amide radical anion were employed. It is expected that this would represent a maximum value (i.e., compare the potentials for the protonated radical acid, $\text{CH}_3\dot{\text{C}}(\text{OH})\text{COOH}$, and amide, $\text{CH}_3\dot{\text{C}}(\text{OH})\text{CONH}_2$, Table VI).

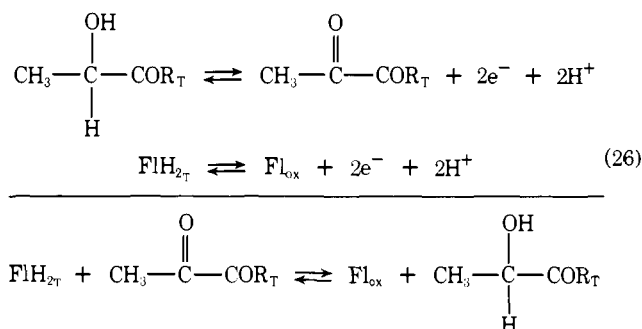
Finally, it is necessary to compute the free-energy differences between the initial and final states. The potential for the $\text{FlH}_2/\text{Fl}_{\text{ox}}$ couple is obtained by summing the calculated half-cell reactions (eq 24). The values obtained (listed in Table



V) are in substantial agreement with published values for the $\text{FlH}_2/\text{Fl}_{\text{ox}}$ couple.^{40,44} The standard potential, E° , for the pyruvate couple has been determined by Burton⁴⁵ from a thermodynamic calculation as +0.2238. A comprehensive compilation of E° values has been prepared by Clark.⁴⁰ The values range from +0.221 to +0.263. Burton's value⁴⁵ of +0.224 was employed in these calculations since the E° values of the other substrates in this study could only be estimated from thermodynamic calculations based on standard free energies of formation. Employing a $E^\circ = +0.253$ changes the ΔE_m between the flavin and pyruvate couples but does not alter the conclusions. In fact, the agreement between the changes observed in $\log k_3$ vs. pH (Figure 10E) is better supported by the more positive E° (see Table V). A reasonable value for pyruvamide was estimated to be $E^\circ = +0.2185$ from thermodynamic free energies of formation ($\Delta G^\circ = 10.08$). Equation 25 provides the proper pH corrections to yield the



E_m values necessary to obtain the free-energy change from initial to final states. In a manner analogous to the determination of the free-energy levels of the radical species, the free energy between the final and initial states is obtained by summing the appropriate half-cell reactions ($\Delta G^\circ = E_m$ 46.1206 at 30 °C for a $2e^-$ process) as shown in eq 26. The

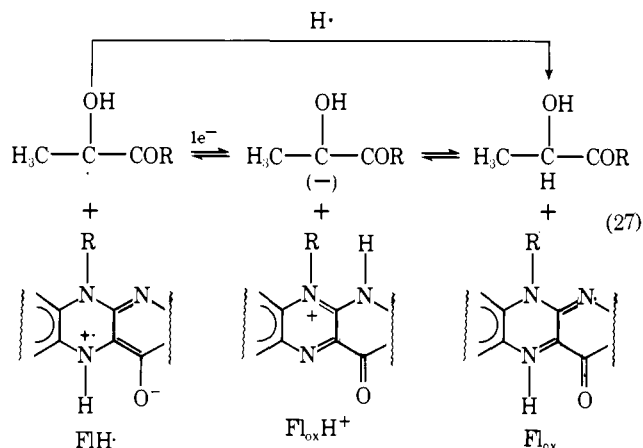


values of ΔG° for the overall reaction are given in Table V for a number of pH's.

The computed standard free energies of formation of intermediates and products have been employed (Figure 11A-C) to construct alternate route reaction coordinate diagrams which involve radical pair intermediates. In Figures 11A and 11C preequilibrium protonation of the carbonyl oxygen is followed by rate determining $1e^-$ transfer from the 1,5-dihydroflavin to yield the $[\text{FlH}\cdot_T \cdot \text{C}(\text{O})\text{OH}]$ pair which then goes on to products via $1e^- + \text{H}^+$ or H \cdot transfer from $[\text{FlH}\cdot_T \cdot \text{C}(\text{O})\text{OH}]$

(vide infra). The computed reaction coordinates predict that a decrease in the rate for $1e^-$ transfer from FlH_2T to $>\text{C}=\text{OH}^+$ should occur with a decrease in pH because the difference in the standard free energy of $(\text{CH}_3\text{-C}(=\text{OH})\text{COOH})_{\text{T}}$ and $(\text{CH}_3\text{C}(\text{OH})\text{COOH})_{\text{T}}$ becomes less negative. It is an experimental fact that the rate constant for $1e^-$ transfer is a function of the potential difference between oxidant and reductant.^{46,47} In Figure 11B $1e^-$ transfer from FlH_2T to $>\text{C}=\text{O}$ yields the radical pair $[\text{FlH}\cdot\text{T}\cdot\text{C}\cdot\text{O}^-]$ which is converted in an encounter controlled proton transfer ($10^9 \text{ M}^{-1} \text{ s}^{-1}$; $\text{p}K_{\text{a}}$ of $\cdot\text{C}\text{-OH} \rightleftharpoons \cdot\text{C}\text{-O}^- + \text{H}^+$ is 9.6⁴²) to the more stable $[\text{FlH}\cdot\text{T}\cdot\text{C}\text{-OH}]$ radical pair which then goes on to products via $1e^- + \text{H}^+$ or $\text{H}\cdot$ transfer. In construction of the reaction coordinates of Figure 11 the rate constants for $1e^-$ and H^+ transfer reactions have been taken as 10^9 s^{-1} in the thermodynamically favored direction^{42,47,48} and the microscopic $\text{p}K_{\text{a}}$ for dissociation of $>\text{C}=\text{OH}^+$ has been reasonably chosen as $10^{+6.49}$ [$\Delta G^\circ = -1.387 (\text{pH} - \text{p}K_{\text{a}})$]. Inspection of the reaction coordinates for pyruvic acid and pyruvamide reveals that either radical species, $\cdot\text{C}\text{-O}^-$ or $\cdot\text{C}\text{-OH}$, could serve as an intermediate since the ΔG° for either pair is less than $\Delta G^{\ddagger}_{\text{exptl}}$ by ~ 12 to $\sim 17 \text{ kcal mol}^{-1}$. The pathways involving protonation of the carbonyl group followed by $1e^-$ transfer on the one hand and $1e^-$ transfer followed by radical anion protonation on the other are the stepwise routes to generation of the neutral radical species. Concertedness in the H^+ and $1e^-$ transfer step yielding $[\text{FlH}\cdot\text{C}\text{-OH}]$ directly must also be considered (Scheme VIII). The concerted reaction requires general acid catalysis and would allow an explanation for the observation of catalysis by pyruvic acid in the reduction of pyruvic acid.

Regardless of the details of proton transfer leading to a radical intermediate, the termination step of the radical mechanism must involve $1e^-$ transfer to provide a carbanion, followed by H^+ transfer or alternatively $\text{H}\cdot$ transfer to provide the carbon acid directly (eq 27). The microscopic $\text{p}K_{\text{a}}$ of the



$\beta\text{-CH}$ moieties of pyruvic acid, pyruvamide, or ethyl pyruvate are unknown. The values of $\Delta G^{\ddagger}_{\text{exptl}}$ for oxidation of lactic acid and pyruvamide (Figure 11A-C) are 23 to 26 kcal mol^{-1} between pH 1 to 7. The ΔG° of formation of the carbanion from a lactic acid derivative will exceed $\Delta G^{\ddagger}_{\text{exptl}}$ in this pH range (carbanion formation forbidden) if the $\text{p}K_{\text{a}}$ of the carbon acid exceeds 25. However, $1e^-$ transfer leading to the intimate ion pair of eq 27 followed by H^+ transfer prior to dissociation of the partners is eminently reasonable. A preference for this mechanism over the kinetically equivalent mechanism of $\text{H}\cdot$ transfer rests on the known propensity for Fl_{ox} to act as a carbanion oxidant (dehydrogenation of dimethyl *trans*-dihydrophthalate,⁵⁰ oxidation of nitroalkanes,⁵¹ and benzyl²⁷). The reversibility of the flavin mediated pyruvate \rightleftharpoons lactate reaction (even below pH 7; ΔG° 1 to 2 kcal) and the fact that this reaction becomes favored at alkaline pH (Experimental Section) are in accord with a carbanion mechanism.

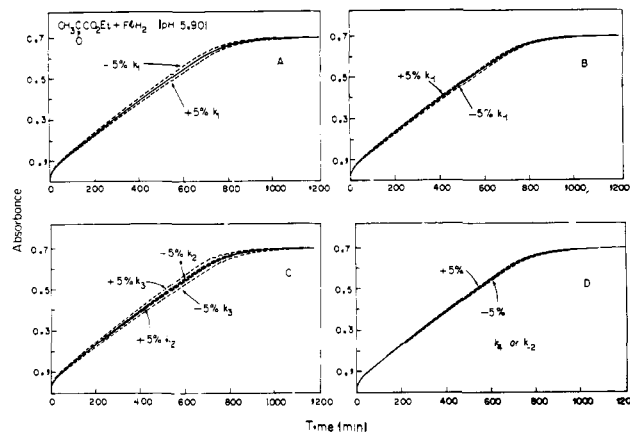


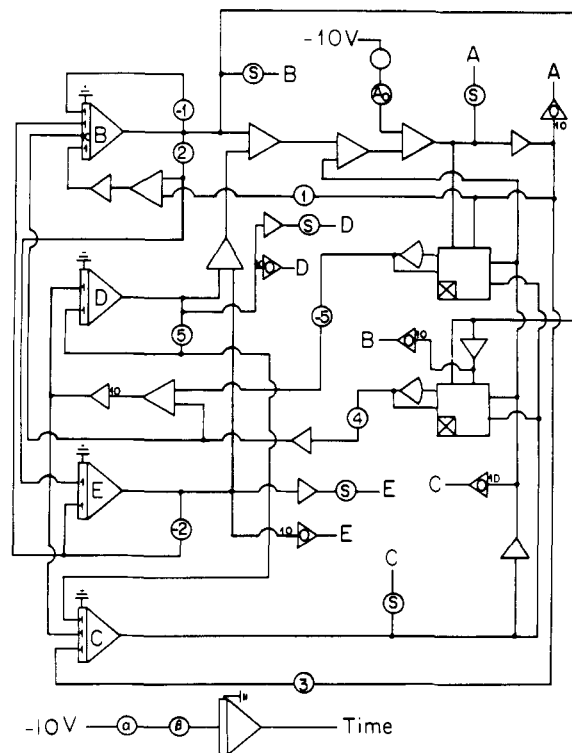
Figure 12. Sensitivity of the analog solution of Scheme II for the reaction of ethyl pyruvate (0.10 M) with 1,5-dihydroflavin-3-acetic acid ($6.5 \times 10^{-5} \text{ M}$).

Acknowledgment. The product analysis for ethyl lactate and a few preliminary experiments employing ethyl pyruvate as the carbonyl substrate were performed by Dr. S. Shinkai (see ref 15). The support of the National Science Foundation (BMS75-22420) and the National Institutes of Health (AM09171-12) is gratefully acknowledged.

Appendix

The conclusions of the present investigation are dependent upon the analog simulation of the differential equations derived from the abbreviated mechanism of Scheme II. The analog solutions were carried out with the program of Scheme IX.

Scheme IX



Although eight individual constants can be varied, the sensitivity of the overall fits of A_{443} vs. time were very good in all cases (some 36 kinetic runs). Figures 12A to 12D represent actual kinetic runs for which the best solution is indicated by a solid line and six of the eight constants have been varied by changing the attenuator pot settings (which represent the actual rate constants) by $\pm 5\%$. The two rate constants not in-

Table VII. Values for the Rate Constants of Scheme III with Ethyl Pyruvate (0.10 M) as the Carbonyl Substrate at pH 5.90 ($\mu = 1.0$, 30 °C)^a

Rate constant	Best solution	Attenuator variation	
		+5%	-5%
$k_1, \text{M}^{-1} \text{min}^{-1}$	8.20×10^{-1}	8.62×10^{-1}	7.78×10^{-2}
k_{-1}, min^{-1}	1.89×10^{-2}	1.98×10^{-2}	1.79×10^{-2}
k_2, min^{-1}	4.94×10^{-2}	5.20×10^{-2}	4.68×10^{-2}
k_{-2}, min^{-1}	2.29×10^{-2}	2.41×10^{-2}	2.18×10^{-2}
$k_3, \text{M}^{-1} \text{min}^{-1}$	1.00×10^{-1}	1.06×10^{-1}	9.53×10^{-2}
$k_4, \text{M}^{-1} \text{min}^{-1}$	3.97×10^3	4.17×10^3	3.77×10^3
k_5, min^{-1}	2.79×10^{-1}	2.93×10^{-1}	2.65×10^{-1}
$k_{-5}, \text{M}^{-1} \text{min}^{-1}$	4.06×10^1	4.24×10^1	3.86×10^1

^a The best analog solution and a $\pm 5\%$ variation of each rate constant is compared to show sensitivity and uniqueness of the analog model solution.

cluded are k_5 and k_{-5} . For these constants a $\pm 5\%$ variation in the attenuators produce lines that are easily discernible as slightly poorer fits. Since $k_5 \gg k_4$ and k_5 is about 100 times k_{-5} the solution is less sensitive to those rate constants which represent the comproportionation reaction of Fl_{ox} plus carbinolamine. In viewing Figure 12, the reader should be aware that the graphical fits were carried out with an x-y recorder employing a 40 × 25 cm plotting area so that the variations are quite sizable. Table VII lists, as an example, the determined rate constants of Scheme III for a particular run and the resultant changes in constants accompanying a $\pm 5\%$ variation of the attenuator pot settings. For the pyruvic acid experiments less than 10% of the parts for any trace of A₄₄₃ vs. time, regardless of pH or pyruvic acid concentration, exhibited deviations from the best solutions of more than 0.005 optical density units. All experiments could be fit within 0.01 OD units (scale 0 to 1.0) for every portion of the curve. Thus, the computer determination of the rate constants for pyruvic acid were within the accuracy of the spectrophotometer.

References and Notes

- Postdoctoral Fellow, Department of Chemistry, University of California, Santa Barbara, Calif.
- T. C. Bruice, "Progress in Bioorganic Mechanisms", E. T. Kaiser and F. J. Kezdy, Ed., Wiley-Interscience, New York, N.Y., 1976, p 1.
- For Part 1, see T. C. Bruice and Y. Yano, *J. Am. Chem. Soc.*, **97**, 5263 (1975).
- R. F. Williams, S. Shinkai, and T. C. Bruice, *Proc. Natl. Acad. Sci. U.S.A.*, **72**, 1763 (1975).
- P. Hemmerich, *Helv. Chim. Acta*, **47**, 464 (1964).
- "Handbook of Chemistry and Physics", R. C. Weast, Ed., Chemical Rubber Publishing Co., Cleveland, Ohio, 1971-72.
- G. Jander and G. Scholz, *Z. Phys. Chem. (Leipzig)*, **192**, 163 (1943).
- H. S. Ankar, *J. Biol. Chem.*, **176**, 1333 (1948).
- R. C. Thomas, C. H. Wang, and B. E. Christensen, *J. Am. Chem. Soc.*, **73**, 5914 (1951).
- E. Leete, L. Marion, and I. D. Spenser, *Can. J. Chem.*, **33**, 405 (1955).
- R. F. Borch, M. D. Bernstein, and H. D. Durst, *J. Am. Chem. Soc.*, **93**, 2897 (1971).
- Y. Pocker, J. E. Meany, B. J. Nist, and C. Zadorojny, *J. Phys. Chem.*, **73**, 2879 (1969).
- H. Strehlow, *Z. Electrochem.*, **66**, 3921 (1962).
- Detection of ethyl lactate as the product has been reported previously by S. Shinkai and T. C. Bruice (see ref 15). The account here is from Dr. Shinkai's determination.
- S. Shinkai and T. C. Bruice, *J. Am. Chem. Soc.*, **95**, 7526 (1973).
- S. B. Smith and T. C. Bruice, *J. Am. Chem. Soc.*, **97**, 2875 (1975).
- S. Ghisla, U. Hartmann, P. Hemmerich, and F. Müller, *Justus Liebig's Ann. Chem.*, 1388 (1973).
- D. Clerin and T. C. Bruice, *J. Am. Chem. Soc.*, **96**, 5571 (1974).
- G. Blankenhorn, S. Ghisla, and P. Hemmerich, *Z. Naturforsch. Teil B*, **27**, 1038 (1972).
- (a) C. Kern and T. C. Bruice, *J. Am. Chem. Soc.*, **98**, 3955 (1976).
- R. F. Williams, S. Shinkai, and T. C. Bruice, *J. Am. Chem. Soc.*, in press.
- R. F. Williams and T. C. Bruice, "The Kinetics and Mechanisms of 1,5-Dihydroflavine Reduction of Carbonyl Compounds and Flavine Oxidation of Alcohols", Part 5.
- (a) J. M. Sayer, M. Peskin, and W. P. Jencks, *J. Am. Chem. Soc.*, **95**, 4277 (1973); (b) J. M. Sayer and W. P. Jencks, *J. Am. Chem. Soc.*, **95**, 5637 (1973).
- V. Massey and Q. H. Gibson, *Fed. Proc., Fed. Am. Soc. Exp. Biol.*, **23**, 18 (1964).
- P. Hemmerich, C. Veeger, and H. C. S. Wood, *Angew. Chem., Int. Ed. Engl.*, **4**, 67 (1965).
- F. Müller, M. Brüstlein, P. Hemmerich, V. Massey, and H. Walker, *Eur. J. Biochem.*, **25**, 573 (1973).
- Part 3: T. C. Bruice and J. B. Taulane, following paper in this issue.
- J. W. Swinehart, *J. Am. Chem. Soc.*, **87**, 904 (1965).
- B. G. Barman and G. Tollin, *Biochemistry*, **11**, 4670 (1972).
- E. J. Land and A. J. Swallow, *Biochemistry*, **8**, 2117 (1969).
- Y. Pocker, J. E. Meany, and C. Zadorojny, *J. Phys. Chem.*, **75**, 792 (1971).
- J. Cashman and T. C. Bruice, unpublished observation.
- L. Wolff, *Justus Liebig's Ann. Chem.*, **317**, 1 (1901).
- (a) E. H. Cordes and W. P. Jencks, *J. Am. Chem. Soc.*, **84**, 832 (1962); (b) *ibid.*, **85**, 2843 (1963); (c) J. E. Reimann and W. P. Jencks, *ibid.*, **88**, 3973 (1966); (d) E. G. Sander and W. P. Jencks, *ibid.*, **90**, 6154 (1968); (e) J. M. Sayer and W. P. Jencks, *ibid.*, **95**, 5637 (1973); F. S. Rosenberg, S. M. Silver, J. M. Sayer, and W. P. Jencks, *ibid.*, **96**, 7986 (1975).
- P. Hemmerich and M. S. Jörns in "Enzymes: Structure and Function", C. Veeger, J. Drenth, and R. A. Gastaban, Ed., North-Holland Publishing Co., Amsterdam, **29**, 95 (1972).
- L. E. Brown and G. A. Hamilton, *J. Am. Chem. Soc.*, **92**, 7225 (1970).
- G. A. Hamilton, *Prog. Bioorg. Chem.*, **1**, 83 (1971).
- I. Yokoe and T. C. Bruice, *J. Am. Chem. Soc.*, **97**, 450 (1975); E. L. Loechler and T. C. Hollocher, *J. Am. Chem. Soc.*, **97**, 3235 (1975).
- T. C. Bruice, L. Hevesi, and S. Shinkai, *Biochemistry*, **12**, 2038 (1973).
- W. M. Clark, "Oxidation-Reduction Potentials of Organic Systems", Robert E. Kreiger Publishing Co., 1972, pp 444, 504.
- R. D. Draper and L. L. Ingraham, *Arch. Biochem. Biophys.*, **125**, 802 (1968).
- P. S. Rao and E. Hayon, *J. Am. Chem. Soc.*, **96**, 1287 (1974).
- P. S. Rao and E. Hayon, *J. Am. Chem. Soc.*, **97**, 2986 (1975).
- L. Anderson and G. W. E. Plaut in "Respiratory Enzymes", H. A. Lardy, Ed., Burgess Publishing Co., Minneapolis, Minn., 1950, pp 71-84; C. Long, Ed., "Biochemists Handbook", Van Nostrand, Princeton, N.J., 1961, pp 85-95.
- K. Burton and H. A. Krebs, *Biochem. J.*, **54**, 94 (1953); K. Burton and T. H. Wilson, *Biochem. J.*, **54**, 86 (1953).
- R. A. Marcus, *Annu. Rev. Phys. Chem.*, **15**, 155 (1964), and references cited therein.
- P. S. Rao and E. Hayon, *J. Phys. Chem.*, **77**, 2753 (1973); **79**, 397 (1975).
- M. Eigen, *Angew. Chem. Int. Ed. Engl.*, **3**, 1 (1964).
- A calculation based on σ_p values yields a $\text{p}K_a \sim -6$ for carbonyl oxygen protonation pyruvic acid and pyruvamide.
- L. Main, G. J. Kasperek, and T. C. Bruice, *J. Chem. Soc., Chem. Commun.*, 847 (1972); *Biochemistry*, **11**, 3991 (1972).
- D. J. T. Porter, J. G. Voet, and H. J. Bright, *J. Biol. Chem.*, **247**, 1951 (1972); **248**, 4400 (1973).